SIMULATED MASS TRANSPORT OF 1,2-DIBROMOETHANE IN GROUNDWATER OF SOUTHEAST ALBUQUERQUE, NEW MEXICO
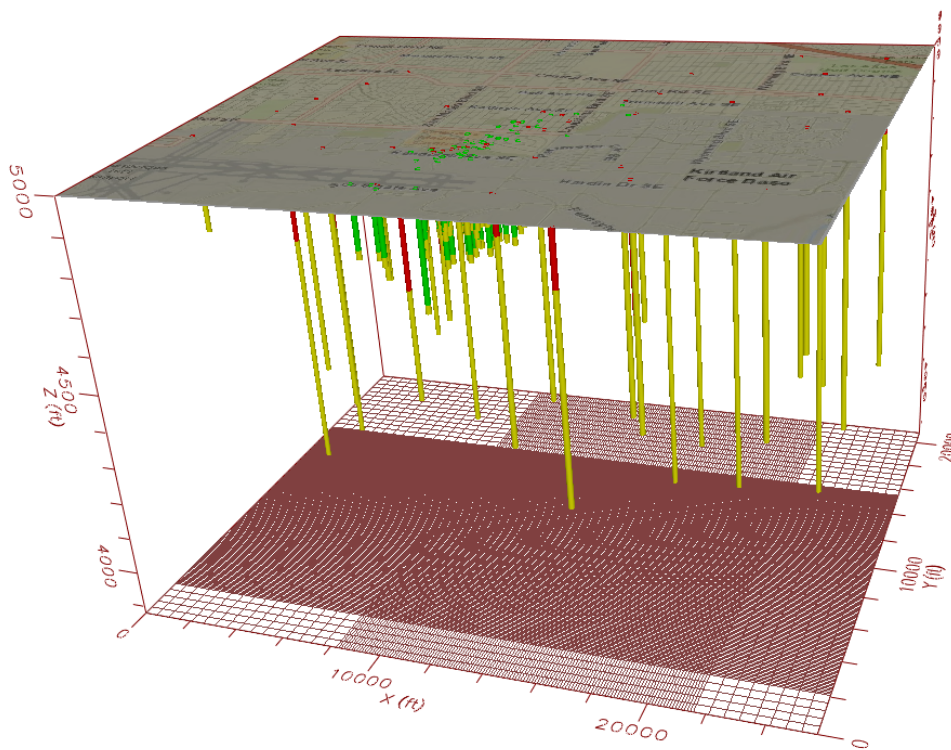
By: Scott Ellinger

United States Environmental Protection Agency

Region 6

Prepared For:

New Mexico Environment Department

Draft Date: September 16, 2013

SIMULATED MASS TRANSPORT OF 1,2-DIBROMOETHANE IN GROUNDWATER OF SOUTHEAST ALBUQUERQUE, NEW MEXICO

By Scott Ellinger

ABSTRACT

A three-dimensional groundwater flow and contaminant transport model was developed to study the mass transport of 1,2-dibromoethane (EDB) in the Santa Fe Group aquifer system of southeast Albuquerque, New Mexico. The model simulates the movement of EDB associated with past releases of aviation gasoline at Kirtland Air Force Base (AFB). EDB ($C_2H_4Br_2$) is a brominated hydrocarbon that tends to be mobile and persistent in groundwater systems. Individuals who consume EDB in excess of the maximum contaminant level (MCL), 0.05 µg/l (or parts per billion), could experience problems with the liver, stomach, reproductive system, or kidneys, and may have an increased risk of cancer.

EDB has migrated thousands of feet from a known source area, the Bulk Fuels Facility at Kirtland AFB, towards drinking water production wells. The regional aquifer (the Santa Fe Group aquifer system) currently provides approximately 60% of Albuquerque's drinking water supply. The Albuquerque-Bernalillo County Water Utility Authority reported that in 2010, ninety-two wells supplied 19.6 billion gallons of drinking water from the aquifer.

The objectives of groundwater modeling were to examine concentrations of EDB that may eventually reach production wells in southeast Albuquerque, and evaluate ways to control plume movement. The computer model utilizes the MODFLOW program for simulating groundwater flow, and a multi-species transport model referred to as MT3DMS for EDB transport. The model also uses ZoneBudget for computing volumetric groundwater flow and Modpath for delineating recovery well capture zones. Groundwater flow was simulated as a steady-state condition and calibrated to regional and local hydraulic head measurements for 2011-2012. EDB transport was simulated by processes of advection and dispersion over a 75-year period.

Results for simulated EDB movement, without using hydraulic controls in the model, showed EDB reaching drinking water supply wells known as Ridgecrest-5 in approximately 30 years, Ridgecrest-3 (~70 yrs), and KAFB-3 (~40 yrs). Results for the VA hospital production well (~2-3 yrs) were less clear, however, possibly because of numerical dispersion. The model also showed potential but less likely impacts to Ridgecrest 2 and Ridgecrest 4, depending on changes to local and regional groundwater gradients as determined by model sensitivity analyses. Concentrations of EDB reaching drinking water production wells were less than 2.0 µg/l.

In most cases, impacts to drinking water production wells at concentrations at the MCL or greater were avoided by placing simulated recovery wells in the model. Recovery wells were placed at: (i) the leading edge of the plume (to the southwest of

EPA United States Environmental Protection Agency

Ridgecrest 5 and Ridgecrest 3); (ii) along the western edge of the plume (near the VA hospital production well); and (iii) just north of the area referred to as the light non-aqueous phase liquid zone (just north of the Bulk Fuels Facility location). Control of the plume near the VA hospital production well was only marginally effective, and hydraulic controls in general were sensitive to changes in groundwater gradients related to changes in hydraulic boundaries.

If a remediation system is implemented that includes hydraulic controls, a groundwater management plan should be included. A plan is needed to monitor the installation of new drinking water production wells and/or changes to existing wells, because new or modified wells may cause changes to the groundwater system overall. Any significant changes in local or regional groundwater gradients could result in the need for a re-evaluation of the hydraulic control designs of the remediation system.

EPA   United States
Environmental Protection
Agency

ACKNOWLEDGEMENTS

EPA United States
Environmental Protection
Agency

TABLE OF CONTENTS

EPA United States Environmental Protection Agency

EPA United States Environmental Protection Agency

ILLUSTRATIONS

(Note: Displays of model output are not limited to the illustrations listed below. Additional maps, cross-sections, plume slices, 3-dimensional diagrams, plume animation, and other illustrations are available to NMED and can be tailored to provide information on specific questions or concerns.)

EPA United States Environmental Protection Agency

LIST OF TABLES

LIST OF EQUATIONS

EPA United States Environmental Protection Agency

ABBREVIATIONS AND ACRONYMS

ABCWUA	Albuquerque-Bernalillo County Water Utility Authority
AFB	Air Force Base
API	American Petroleum Institute
ASTM	American Society of Testing and Materials
AVGAS	aviation gasoline
BFF	bulk buels facility
bls	below land surface
CSIA	compound specific isotope analysis
EDB	1,2-dibromoethane
EPA	Environmental Protection Agency
ft	feet
GHB	general head boundary
gpm	gallons per minute
JP-4	jet propellant-4
JP-8	jet propellant-8
K	hydraulic conductivity
KAFB	Kirtland Air Force Base *(used as prefix to well numbers; e.g., KAFB-15)*
LNAPL	light non-aqueous phase liquid
m	meters
msl	mean sea level
NAPL	non-aqueous phase liquid
NMBGM	New Mexico Bureau of Geology and Mineral Resources
NMED	New Mexico Environment Department
NMGS	New Mexico Geology Society
NWIS	National Water Information System
QA	Quality Assurance Project Plan
RMS	root mean squared
USGS	U.S. Geological Survey
VA	Veterans Administration

EPA United States Environmental Protection Agency

1. INTRODUCTION

1.1.   Overview

The U.S. Environmental Protection Agency (EPA) has prepared a groundwater flow and contaminant transport model to evaluate the mass transport of 1,2-dibromoethane (EDB) (also known as dibromoethane, ethylene dibromide, and other names), in the Santa Fe Group aquifer system in southeast Albuquerque. The computer model was developed at the request of the New Mexico Environment Department (NMED). The main purpose for the model is to provide a greater understanding of EDB movement in groundwater north of Kirtland Air Force Base (AFB), and more specifically, to examine plume movement towards drinking water supply wells including wells in the Ridgecrest well field, the VA hospital production well, and wells owned by Kirtland AFB. In addition, the model was used to evaluate initial pumping designs for creating capture zones to control plume movement and reduce EDB concentrations. This report provides a detailed account of all aspects of model development, includes project results and conclusions, and explains modeling uncertainties and sensitivities in relation to their significance to project goals and conclusions. The model may be updated in the future depending on the availability of new or additional data and related needs.

The study area, or model domain, encompasses 11,205 acres of southeast Albuquerque and extends 4.8 miles east to west, and 4.0 miles north to south (figs. 1 and 2). Many factors were considered in determining the size and position of the model domain. These included the distribution of drinking water production wells and groundwater monitoring wells across southeast Albuquerque, the size of the contaminated area, the distance between the Bulk Fuels Facility (BFF) and the Ridgecrest well field, the need to have a domain size providing sufficiently detailed output, and other similar factors. The edges of the model domain also have an important numerical purpose; they were assigned as numerical groundwater flow boundaries that provide hydraulic connections between the model domain and the basin-wide groundwater flow system.

Vertically, the model includes the interval of the upper and middle parts of the Santa Fe Group aquifer system between 5,000 ft above mean sea level (msl) to 3,880 ft

msl, for a total thickness of 1,120 ft. The Albuquerque-Bernalillo County Water Utility Authority (ABCWUA), the Veterans Administration (VA) hospital, and Kirtland AFB withdraw groundwater from wells screened at various depths within this section of the Santa Fe Group aquifer system.
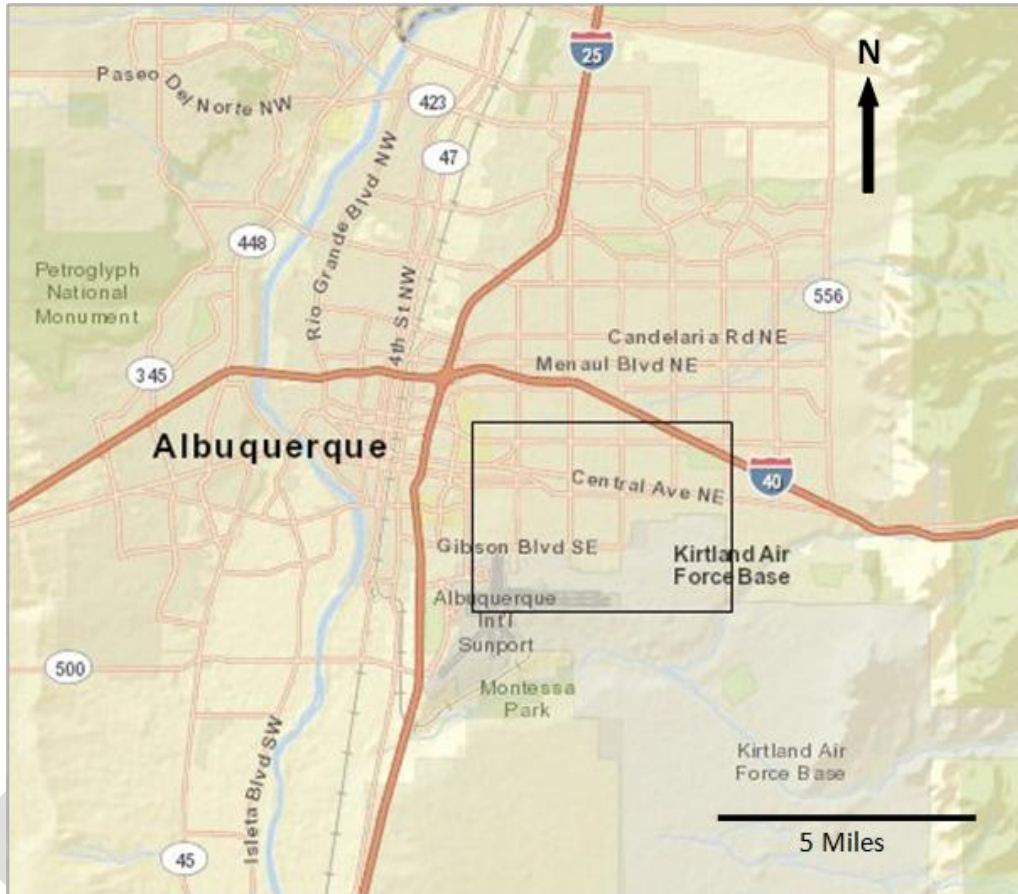
Figure 1: Location of model domain in southeast Albuquerque.
Domain outlined by black rectangle.

The model includes both groundwater flow and mass transport components integrated into a single modeling environment through a commercial data processor. The data processor is Visual Modflow Pro, version 2010, from Schlumberger Water Services Inc. Groundwater flow modeling was accomplished with the MODFLOW program (Harbaugh and others, 2000) for simulating three-dimensional groundwater flow. MODFLOW was used with a modular three-dimensional multi-species transport model, referred to as MT3DMS (Zheng and Wang, 1999), to simulate advective transport of

EPA United States Environmental Protection Agency

EDB. Additional computer programs employed were Modpath (Pollock, 1994) for particle tracking, and ZoneBudget (Harbaugh, 1990) for calculating groundwater volumetric flow. Supplemental hand calculations were made when necessary to derive various numerical input values.
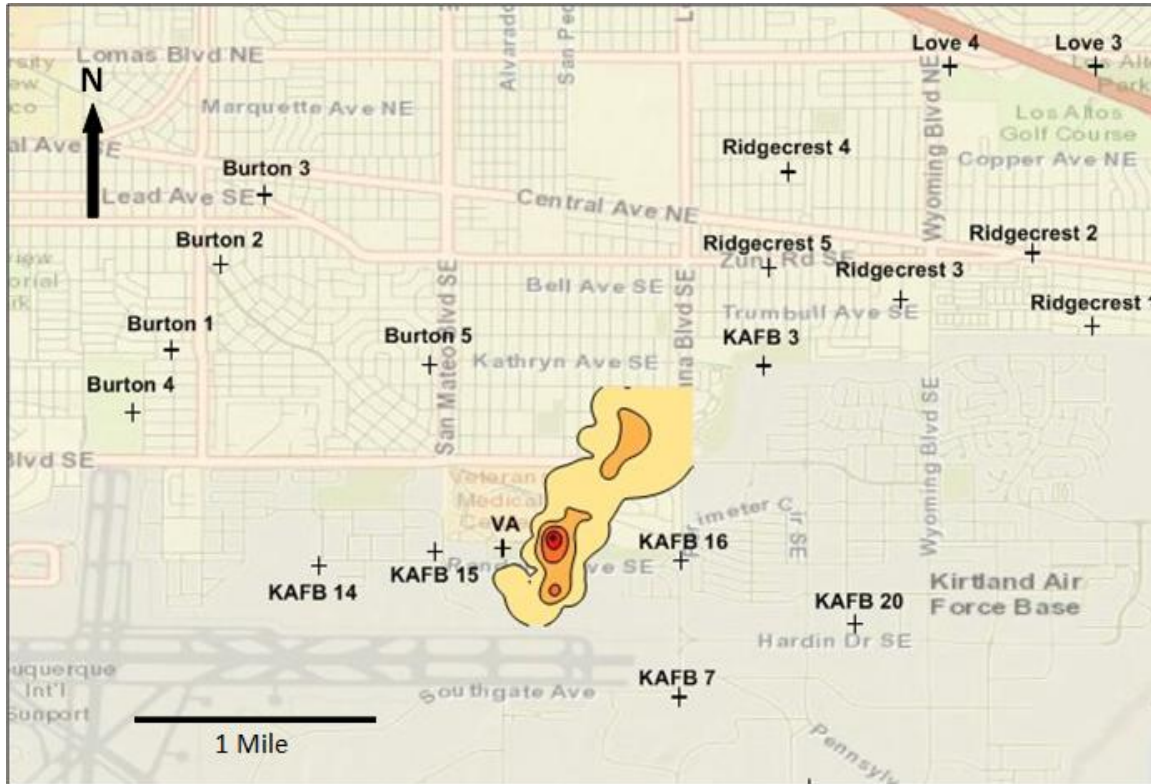
Figure 2: Enlarged map of model domain.
Current EDB contamination shown in relation to drinking water supply wells. Plume contouring based on 4th quarter 2011 data for the shallow zone. Outside edge 0.05 μg/l EDB; higher concentrations (red) up to 190 μg/l.

An approved comprehensive Quality Assurance and Quality Control (QA/QC) Project Plan governed model construction and application. One element of the QA/QC project plan calls for technical reviews of the model. Model reviews were conducted by EPA Region 6 and NMED, Schlumberger Water Services Inc., and related consultations were provided by the EPA Robert S. Kerr Environmental Research Center in Ada, Oklahoma. A QA/QC review was provided to the Region 6 Quality Assurance Officer at the end of the project to ensure that all applicable QA/QC requirements were met.

1.2. Problem Definition

The BFF reportedly operated from 1951 to 1999 for the purposes of fuel storage, processing, and shipping and receiving (Shaw Environmental and Infrastructure, 2012). During this period, undetermined amounts of fuel were released from underground pipelines and recent estimates by NMED suggest the amounts could have been up to approximately 24 million gallons. During the 1951 to 1999 period, fuels handled at the facility included aviation gasoline (AVGAS), jet propellant 4 (JP-4), and jet propellant 8 (JP-8). These fuels have migrated approximately 500 ft down through the vadose (unsaturated) zone to reach the regional water table at the top of the Santa Fe Group aquifer system. The Santa Fe Group aquifer system is heavily used to supply drinking water to the City of Albuquerque. ABCWUA reported that in 2011, ninety-two wells supplied 19.6 billion gallons of drinking water from the aquifer (ABCWUA, 2011). Contamination from the BFF consists of petroleum related compounds which are present in the vadose zone, and in groundwater as both light non-aqueous phase liquid (LNAPL) and dissolved constituents. One of the most toxic compounds present is EDB, which has migrated as a dissolved constituent approximately 6,500 ft from the source area towards drinking water supply wells.

Site remediation and subsurface investigations are currently taking place under the direction of the NMED Hazardous Waste Bureau. Kirtland AFB is performing soil vapor extraction to remove fuel from the vadose zone, and over one-hundred groundwater monitoring wells have been installed. Most hydrocarbons appear to be naturally attenuating but it is unclear whether natural attenuation of EDB is occurring. A cursory review of EDB concentrations in monitoring wells conducted by EPA suggests that EDB attenuation is either not occurring or is occurring very slowly.

The main direction of movement of the EDB plume is to the northeast. EDB moves along groundwater gradients caused by pumping wells under the processes of advection and dispersion. Less likely transport processes are sorption and chemical reactions. The nearest ABCWUA wells are located in the Ridgecrest well field, and Ridgecrest wells 5 and 3 are approximately 1-mile from the estimated plume front (i.e., downgradient extent of EDB) (fig 2). The exact location of the front is not known but

estimated from using available data and contouring algorithms. There are other wells around the plume's perimeter that are closer, however, which include the VA hospital production well (several hundred feet west of the plume), and KAFB wells 15, 16, and 3 which provide drinking water to the base and are within approximately one-half mile of the plume. EDB has not been detected in these water production wells so far.

Because of the complex processes involved with contaminant transport, it is extremely difficult to predict impacts to drinking water supply wells without performing an advanced technical analysis using a robust numerical model. Numerical models are powerful tools when enough site-specific high-quality data are available and when the modeling process from system conceptualization to final output is properly executed. Rather than relying on simple predictions, the approach uses tested and validated computer modeling programs that rely on solving partial differential equations, including terms for the predominant mass transport processes. When the equations are solved concentrations in time and space can be accurately determined. For example, the change in concentration over time $(\frac{\partial C}{\partial t})$ in a one-dimensional groundwater flow system, can be described by calculating terms for dispersion, advection, sorption, and chemical reaction as shown in Equation 1. This type of equation must be solved in three-dimensions to predict impacts to drinking water wells from EDB in southeast Albuquerque. The governing equations for three-dimensional mass transport in groundwater may be found in Zheng, 1990.

Equation 1: One-dimension contaminant transport equation.
(Fetter, 2008)

$$\frac{\partial C}{\partial t} = D_L \frac{\partial^2 C}{\partial x^2} - v_x \frac{\partial C}{\partial x} - \frac{B_d}{\theta} \frac{\partial C^*}{\partial t} + \left(\frac{\partial C}{\partial t} \right)_{rxn}$$

$$\text{(dispersion)} \qquad \text{(advection)} \qquad \text{(sorption)} \qquad \text{(reaction)}$$

C: concentration of solute in liquid phase
t :   time
D_L: longitudinal dispersion coefficient
v_x :   average linear groundwater velocity

B_d :   bulk density of aquifer
θ :   volumetric moisture content of porosity for saturated media
C^*:   amount of solute sorbed per unit weight of solid
 rxn: subscript for biological or chemical reaction of solute (not sorption)

All models have certain limitations that affect accuracy and usefulness. Hydrogeology and mass transport are inherently complex and models cannot exactly represent groundwater systems or mass transport processes. The usefulness of a model depends on having enough appropriate data to represent the system or processes being simulated, and how well mathematical treatment of site parameters and variables can approximate the physical system. Results for this model should be kept in perspective by comparing calculated results with what is actually known about the area of concern in southeast Albuquerque.

1.3.   Project Goals

Early in the project NMED provided EPA with two project goals:

- Goal 1: Predict the concentrations of EDB that would be expected to reach production wells (i.e., ABCWUA, KAFB, and VA wells) if nothing was done to mitigate the problem, and;

- Goal 2: Model a capture zone of two proposed extraction wells associated with an LNAPL containment system.

In order to assess whether enough appropriate data existed to support model development and accomplish these goals, EPA thoroughly reviewed available regional and local geologic and hydrogeologic information and Kirtland AFB site investigation data. Subsurface data were obtained from Kirtland AFB site investigation reports, the U.S. Geological Survey (USGS), the ABCWUA, the New Mexico Bureau of Geology and Mineral Resources (NMBGMR), the New Mexico Geology Society (NMGS), and other sources. Groundwater monitoring wells installed during the Kirtland AFB site investigation provided hydraulic head data necessary for groundwater flow model calibration, and groundwater sampling and analysis has provided contaminant concentrations useful for establishing EDB transport conditions. The site investigation has also provided hydraulic conductivity data from slug testing in the EDB plume area,

and hydraulic conductivity data was also available at city well fields from pumping tests reported by ABCWUA and its consultants. Well construction and pumping rates for city wells were also available from ABCWUA. Because of the availability of the necessary modeling data, it was determined that Goal 1 could be accomplished.

Because of limitations of the governing equations used in mass transport modeling, Goal 2 was not accomplishable for LNAPL. Specifically, attempting to model the capture zone of a proposed LNAPL containment system would exceed the capabilities of the governing equations used by MT3DMS. While it is possible to model the groundwater flow field created by extraction wells using MODFLOW, the governing equations of MT3DMS cannot model LNAPL transport. MT3DMS is designed for contaminants dissolved in groundwater. To remain within mathematical capabilities, Goal 2 was reconsidered so that capture would be evaluated for dissolved contamination only (specifically EDB), not LNAPL.

1.4. Quality Assurance

The EPA Quality System defined in EPA Order CIO 2105.0 (formerly 5360.1 A2) *Policy and Program Requirements for the Mandatory Agency-wide Quality System*, includes coverage of environmental data produced from models. Environmental data includes any measurement or information that describe environmental processes, locations, or conditions; ecological or health effects and consequences; or the performance of environmental technology. A combined QA/QC Project Plan was prepared for this project in accordance with EPA's Guidance for modeling (U.S. EPA, 2002). This guidance describes the nature of QA/QC planning for modeling including the relationship to model development and application.

A QA/QC Project Plan is a formal document describing in comprehensive detail the necessary quality assurance, quality control, and other technical activities that must be implemented to ensure that results of work performed will satisfy stated performance criteria. The plan prepared for this project has undergone peer review and was subject to revisions before final approval. The main elements of the QA/QC Project Plan address project management (including quality objectives and criteria for model input and

output), measurement and data acquisition (including model calibration), project assessment and oversight, and data validation and usability.

2. CONCEPTUAL MODEL

A conceptual model is an interpretation or working description of the characteristics and dynamics of the physical and chemical system that lays the foundation for a computer model. Conceptual models rely primarily on existing data. Data gathered for a conceptual model must be carefully reviewed, analyzed, and converted into appropriate input files for the numerical model.

2.1. Sources of Information

Published and unpublished reports on the geology, hydrogeology, and groundwater conditions of the Albuquerque vicinity were reviewed for the conceptual model. On a regional scale, numerous published reports are available from the USGS, NMBGMR, NMGS, and other organizations that provide thorough descriptions of basin-wide geology and hydrogeology. Although most of these reports cover areas much larger than southeast Albuquerque, they are still important because the model domain must be considered in the context of basin-wide hydrogeology. This is especially true with regard to the presence of natural and man-made features located outside the model domain but affecting groundwater flow inside the model domain (i.e., distant hydraulic boundaries). Geologic literature was reviewed for geologic structure, depositional environments, stratigraphy, lithology, and other information. Hydrogeologic literature was reviewed for regional groundwater flow directions, aquifer properties, hydraulic boundaries, and other information.

Although regional studies were used as much as possible, detailed information about the main area of concern was required. Site-specific information was obtained from Kirtland AFB site investigation reports and other reports available on the Kirtland and NMED websites. The most important site-specific information consisted of groundwater level (total head) measurements, EDB concentrations including vertical and horizontal distributions of EDB, and pumping test and slug test data. Locations of drinking water wells, well production rates, well screened intervals, and pumping schedules are also critical to model function. Sources of these data were technical reports and personal communications from ABCWUA, Kirtland AFB, USGS, and NMED.

United States
Environmental Protection
Agency

Information was also necessary on the physical and chemical properties of EDB and its characteristics of mobility in groundwater. That information was obtained from existing research by the EPA (Wilson and others 2008), the American Petroleum Institute (API) (Aronson and Howard, 2008), and the USGS (Katz, 1993); journal articles including McKeever and others (2012), Henderson and others (2009), Falta (2004); and other federal agencies including the Centers for Disease Control and Prevention (2007), and the National Institutes of Health (2011). Site investigation reports by Kirtland AFB provided data for calculating estimates for EDB sorption and decay, and supplied EDB concentration data for establishing model concentration boundaries and properties.

For groundwater flow, the most important data affecting model setup consisted of (i) data on pumping wells and groundwater monitoring wells, (ii) data regarding physical properties of aquifer sediments and in particular the distribution of hydraulic conductivity throughout the model domain, and (iii) the influence of physical flow boundaries occurring outside the model domain. The most important data affecting setup of the mass transport model were: (i) aquifer properties, (ii) existing EDB concentrations, (iii) data on processes of dispersion, sorption, and decay, and (iv) EDB concentrations near the LNAPL/dissolved phase plume interface.

The information sources noted above provided adequate information and data on a sufficient basis so that model development could proceed. Data reports were cross-checked when possible to facilitate the consistency and quality of model input data.

2.2. Geologic and Hydrogeologic Setting

2.2.1. Albuquerque Basin

The model domain lies within a topographically low region known as the Albuquerque basin. The Albuquerque basin is one of a number of geologic basins that occur along the Rio Grande rift and was formed by subsidence along faults occurring mainly along the eastern and western basin margins. The Rio Grande rift was superimposed upon older structures of the Colorado Plateau and the Rocky Mountains (Woodward, 1982), and has been described by Thorn and others (1993) as an area of crustal extension originating in central Colorado and continuing for more than 600-miles south through New Mexico to south of the Mexico/Texas border.

A series of north to south trending basins, including the Albuquerque basin, compose the central part of the rift. Basins of the Rio Grande rift include the Upper Arkansas Valley in Colorado, the San Luis basin, the Española basin, the Santo Domingo basin, and the Albuquerque-Belen basin; and south of the City of Socorro the rift consists of three small basins including the San Marcial, Engle, and Palmos basins (Kelley and others, 1976). A number of published reports consider the Santo Domingo basin and the Albuquerque-Belen basin as a single basin, called the Albuquerque basin.

The Albuquerque basin is the third largest basin in the Rio Grande rift. It is approximately 100-miles long from north to south and approximately 35-miles wide, and covers about 3,060-square miles (Thorn and others, 1993). The east side of the basin is bordered by a 72-mile long line of west-facing fault escarpments made up of four contiguous uplift fault blocks. These uplifted blocks are the Los Pinos, Manzano, Manzanita, and the Sandia mountains. The western border of the Albuquerque basin is an area of relatively low relief compared to the east, and has had little or no faulting at the margin. The northern end is formed mainly by the Jemez uplift and the Nacimiento uplift, and the southern end is the Socorro constriction formed by convergence of the east and west borders (Kelley, 1977).

2.2.2. Santa Fe Group Aquifer System

The Albuquerque basin contains thousands of feet of basin fill consisting mainly of clay, silt, sand, and gravel sized material deposited under a variety of conditions. These deposits are known as the Santa Fe Group which contains the main aquifer in the basin. Thorn and others (1993) reported that sediment thickness in the central part of the basin south of Albuquerque is probably over 14,000 feet thick.

The Santa Fe Group has been divided into three units. In ascending stratigraphic order these are: a lower gray formation, a middle red formation, and an upper buff formation. The lower gray formation occurs below the range of most water supply wells in Albuquerque. The middle red formation is volumetrically the largest component of the Santa Fe Group in the Albuquerque basin, and the upper buff formation is the youngest basin fill unit (Connell and others, 1998). The upper buff formation is a mixture of well

sorted and poorly cemented sand and gravel including beds of silty sand and clay. The upper buff formation was deposited by broad fluvial systems of the ancestral Rio Grande and its tributaries. In a study of core samples taken from the upper 1,500 feet of the Santa Fe Group in the Albuquerque west mesa, the 98th Street site, nearly the entire stratigraphic sequence is reported as having been deposited in a fluvial environment with coarse-grained intervals reflecting deposition in river channels and finer-grained intervals representing overbank and flood plain deposits (Allen and others, 1998). The name Sierra Ladrones Formation has also been used as a name for the upper buff formation (Connell et al. 1998). The upper-most unit of the upper buff formation is called the Ceja Member, which usually occurs above the water table.

Similar to the divisions of lithologic units, the Santa Fe Group aquifer system has been divided into individual hydrostratigraphic units. They are the lower, middle, and upper parts of the Santa Fe Group, and overlying valley and basin fill deposits. The upper part of the Santa Fe Group is the main sedimentary unit addressed by this model. The upper part of the Santa Fe Group is divided into upper and lower unnamed members in Connell and others (1998), based upon stratigraphic correlations from geophysical logs. Kelley (1977) reported that based on well cuttings and stratigraphic sections, the upper Santa Fe Group is coarser and more gravelly in most areas than deeper parts of the Santa Fe Group. The most productive part of the Santa Fe Group aquifer system is the upper part, and the most productive lithologies are paleochannels of the ancestral Rio Grande and, to a lesser extent, pediment-slope and alluvial fan deposits.

Pre-development regional groundwater flow directions of the Santa Fe Group aquifer between Cochiti Lake and San Acacia have been described by Bexfield and Anderholm (2000) for the upper 300 feet of saturated Santa Fe sediments. Their report points out that among the information critical to a thorough understanding of the groundwater flow system, are water level data that indicate the directions of groundwater flow prior to major groundwater withdrawals taking place. They report that prior to 1955, most city wells were completed in the present-day inner Rio Grande valley and the effects of development on regional water levels were limited until the 1960s and 1970s when many additional wells were installed outside the Rio Grande valley, causing effects

over a much wider area. Bjorklund and Maxwell (1961) reported the average pumping rate increased from about 2 million gallons per day in 1930, to about 33 million gallons per day in 1959. Kelly (1982) presented several predevelopment groundwater flow maps in describing the history of groundwater use in Albuquerque, and reported that a major expansion of the municipal well system began in 1959 when several new well fields were developed. Maps of predevelopment groundwater flow covering the area of interest for this model show flow directions mainly being towards the west-southwest.

Development of groundwater resources in the Albuquerque area have resulted in significant changes to groundwater flow directions. Groundwater flow directions in the 1960s do not indicate a northeast flow from the BFF towards production wells, except for the area relatively close to the Love well field. Installation dates for certain early wells in the Love well field are 1954 for Love 1, and 1958 for Love 3, 4, and 5 (Bexfield and others, 1999). The effects of these wells can be seen on maps in Bjorklund and Maxwell, 1961. Wells in the Ridgecrest well field were installed in the 1970s, except for Ridgecrest 5 which was installed in 1990. Although there have been variations in pumping rates at individual ABCWUA and Kirtland AFB wells over the years, groundwater directions in southeast Albuquerque appear to have been towards production wells northeast of the BFF for at least the last several decades.

2.2.3. Ancestral Rio Grande Deposits

A number of drinking water production wells in southeast Albuquerque, including wells in the Ridgecrest well field, some Kirtland AFB wells, and the VA hospital production well, are believed to be screened in sediments deposited by former stream channels of the Rio Grande. These ancestral Rio Grande deposits are important to the model because they are the most productive sediments of the Santa Fe Group aquifer, and the EDB plume is most likely moving through these highly conductive sediments towards drinking water production wells.

In describing geologic history and basin stratigraphy, Hawley and Haase (1992) report that a through-flowing ancestral Rio Grande, including two ancestral tributaries (the Rio San Jose and Rio Puerco), joined the Rio Grande and formed a large

aggradational plain in the central basin. These ancestral Rio Grande deposits are interbedded with piedmont-slope deposits which together form upper Santa Fe Group. The basin floor fluvial deposits are reported as consisting of ancestral river sediments of thick zones (usually less than 1,000 ft) of clean sand and pebble gravel, and the piedmont-slope deposits are reported as poorly sorted and weakly stratified with a silt-clay matrix.

Hawley and Haase (1992) show that the ancestral Rio Grande channel facies is oriented approximately north to south extending through southeast Albuquereque. The following observations regarding hydraulic conductivity and the ancestral Rio Grande deposits were made by Thorn and others (1993): (i) hydraulic conductivity is low east of the eastern limit of the ancestral Rio Grande deposits, (ii) hydraulic conductivity is high west of the eastern limit, and (iii) hydraulic conductivity is low west of the Rio Grande fault. These boundaries place the ancestral Rio Grande deposits and thus a zone of relatively high hydraulic conductivity within the model domain. In addition to the occurrence of these deposits in the model domain, their north to south orientation is also important because the model's finite-difference grid should be oriented along the principal axis of hydraulic conductivity (i.e., north to south).

Data from well-bore flow logging indicate some vertical intervals of the Santa Fe Group aquifer are more productive than others. In a study of six production wells by Thorn (2000), using an impeller-type flow meter measuring flow rates from discrete vertical intervals, higher water production was noted from layers of gravel and sand with varying amounts of sandy clay. The production well located closest to the model domain, Love 6, which is located just to the north, showed two zones of higher production: 900-930 ft (100-150 gallons per minute (gpm)), and 1,030 to 1,050 ft (125-175 gpm). By comparison, flow log results reported for intervals consisting mainly of clay are reported as showing minimal to no flow contribution to the well.

A flow-meter log of well Griegos-1, located northwest of the model domain and near the Rio Grande, showed the most productive zones at 360-380 ft and 540-560 ft below land surface (Thorn, 2001). Bexfield and others (2011) reported on flow logging for Yale-2, located just west of the model domain, under ambient and pumping

conditions. They reported that the highest rates of flow under ambient conditions occur at approximately 656 feet below land surface (bls), and under pumping conditions the greatest flow occurs in the upper parts of the well screen at approximately 558 feet bls or above.

2.3.   Hydraulic and Mass Transport Boundaries

The model requires the specification of boundary conditions for both groundwater flow and contaminant transport. Boundaries represent actual features situated in and around a model domain that have significant influences on groundwater flow and contaminant transport. These include hydrogeologic features, groundwater divides, contamination sources, etc. Groundwater flow boundaries can lie within a model domain, around the perimeter of a domain, or link the model domain to external hydrology. Sizes of contaminant transport boundaries are usually more limited than groundwater flow boundaries because the extents of aquifers are typically much greater. Boundaries must be defined numerically for the governing partial differential equations used by MODFLOW and MT3DMS to be solved.

2.3.1. Groundwater Flow Boundaries

The main natural groundwater flow boundaries affecting the model lie outside the model domain. These include the Rio Grande river (approximately six miles west of the EDB plume), the aquifer/basin edge contact (approximately three miles east), and Tijeras Arroyo just to the southeast. Located also to the south is the perched zone on Kirtland AFB that merges with and supplies water to the regional aquifer. The perched zone reportedly resulted from Kirtland's past water management practices and is not a natural flow boundary (Balleau Groundwater, Inc., 2002). A number of faults are present in the vicinity including the Sandia fault and the Rio Grande fault, but their effects on groundwater flow are unclear (NMED staff, personal communication). No vertical recharge is included in the model and the water table is not used as a flow boundary.

Normally, it is desirable to develop a groundwater flow model with model boundaries corresponding to locations of actual boundaries. This approach was

EPA   United States
Environmental Protection
Agency

attempted during early phases of the project and the boundaries discussed above were included, but the domain was later reduced to a smaller and more focused area. The domain was reduced because there were too many areas lacking sufficient hydrogeologic data to support the level of detail needed for this model. It was decided that a smaller domain with a greater density of data points would be more effective at accomplishing project goals. The initial and final model domains are shown below in figure 3.
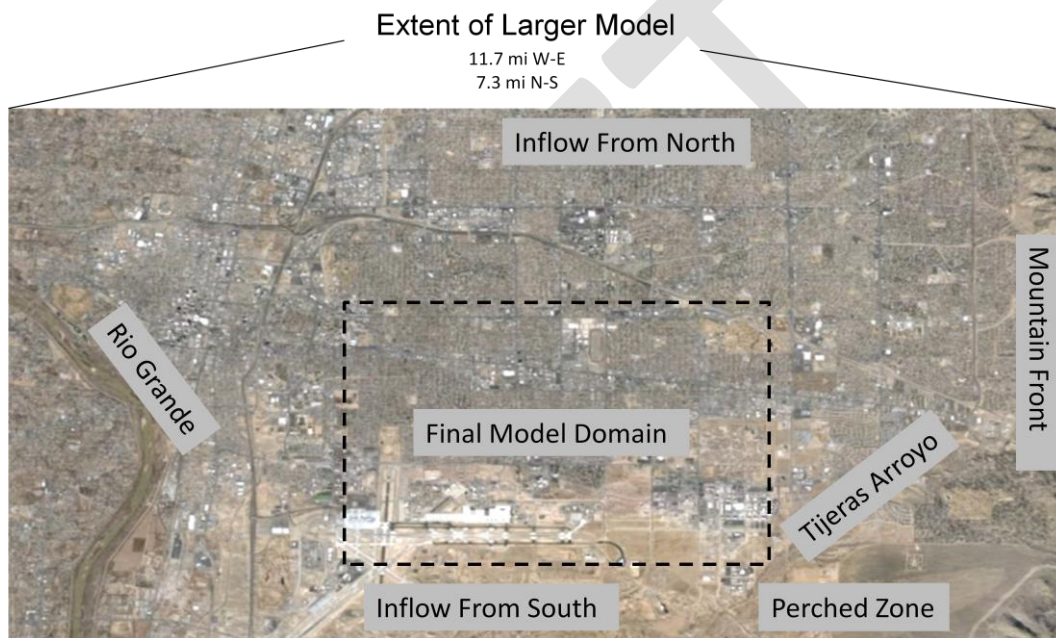
Figure 3: Early model domain showing important basin hydraulic features.
Final model domain shown by dashed outline.

The early larger domain was useful in preliminary modeling because it provided a greater understanding of how the Rio Grande, the mountain front region, Tijeras Arroyo, and the perched aquifer affected groundwater flow. As pointed out by the American Society of Testing and Materials (ASTM), 2008a, it is important to understand the location and conditions of the boundaries and their effects even if lateral boundaries are far from the main area of interest. Hydraulic head used for boundary values in the larger domain were derived from the USGS National Water Information System (NWIS) for the dates December 2011 to February 2012, and from water levels estimated from the groundwater map by Faulk and others (2011). City well pumping rates in the larger

EPA United States Environmental Protection Agency

domain corresponded to December 2011 to February 2012 and were provided by ABCWUA. Information on the Kirtland perched zone was found in Van Hart (2003). Preliminary modeling using the larger model domain did not advance to the point of including mass transport. However, it did provide initial estimates of hydraulic head useful for constructing the smaller, final model domain.

Anderson and Woessner (1992) refer to a certain type of hydraulic boundary as an artificial boundary. Artificial boundaries are commonly used when there are no actual physical boundaries in a model domain. In these cases, boundary values are defined from data on the configuration of the groundwater flow system such as water table maps. Because there are no obvious physical boundaries present in the final model domain, the use of artificial boundaries is appropriate, and necessary for the model to function. If placed around the edges of the final model domain, the boundaries conceptually (and numerically) link groundwater flow in the final model domain to groundwater flow outside the model domain.

Artificial boundaries function according to the type of hydraulic boundary they represent. Franke and others (1987) list the seven most common types of boundary conditions encountered in groundwater systems. They are: constant head, specified head, streamline or stream surface, specified flux, head dependent flux, free surface, and seepage surface. Of these types, the most appropriate hydraulic boundary for use in this model is a specified head boundary. By using specified head boundaries, water levels can be specified as a function of position and time along each border of the model domain. The time value is not relevant for this model, however, because the groundwater flow model is a steady-state model and groundwater flow conditions are constant.

2.3.2. Contaminant Transport

The conceptual site model by Shaw Environmental and Infrastructure, Inc., 2011 (Chapter 7, Section 7.4) describes how non-aqueous phase liquid (NAPL) reached the water table based on measurements of total petroleum hydrocarbons, benzene, and contamination footprints near the water table. It is reported that NAPL migrated 400-500 ft downward through the vadose zone with little or no horizontal spread until it reached

EPA United States Environmental Protection Agency

the water table. At the water table, NAPL began to spread horizontally and mainly to the northeast towards drinking water supply wells including KAFB-3 and the Ridgecrest well field. Fluctuation in the water table elevation has also caused NAPL smearing. NAPL is believed to be trapped below the water table, and will probably be a persistent source of groundwater contamination for the indefinite future.

Kirtland AFB has grouped EDB concentration data for the dissolved phase into three depth zones: shallow, intermediate, and deep. The shallow zone is the zone monitored across the water table and extends 5 to 10 ft below the water table; the intermediate zone extends 15-30 ft below the 2009 water table elevation; and the deep zone extends 30 to 100 ft below the 2009 water table elevation (Shaw Environmental and Infrastructure, Inc., 2011). EDB concentrations are highest in the shallow zone, followed by the intermediate zone, and lowest concentrations are in the deep zone. These discrete depth zones provided logical divisions for establishing initial contaminant conditions in the aquifer using data sets for each zone. These descriptions indicate that two different representations of EDB are needed for the model:

1. A contaminant boundary representing the concentration of EDB in groundwater adjacent to the NAPL area (referred to as LNAPL for this model), providing a source of EDB to the dissolved phase plume, and

2. A representation of the horizontal and vertical distribution of EDB concentrations in the aquifer forming the EDB dissolved phase plume.

While the LNAPL/EDB source can be included as a contaminant boundary condition, the distribution of EDB concentrations throughout the aquifer can be handled as an aquifer property to define existing conditions in the aquifer at the start of a model run.

One approach to the EDB source boundary is to specify a contaminant boundary approximately the same size and shape as the LNAPL area and containing EDB concentrations that are declining over time. Simulated declining concentrations would account for possible concentration reductions caused by site remediation. The boundary concentration can be set to decrease by a certain percentage, such as 10% per year. Assuming that the concentrations of EDB partitioning from fuel to groundwater are much less than EDB concentrations in aviation gasoline, concentrations therefore occurring in the shallow zone can be used to approximate starting contaminant source boundary

concentrations. The highest concentrations reported in the shallow zone are approximately a few to several hundred micrograms per liter in 2011-2012. By comparison, concentrations of EDB in aviation gasoline have been reported to be 444 mg/l (Spidle and others 2007), 600 mg/l (Falta, 2004), and less than 4 ml/gal (2,377 mg/l) (Chevron, 2003).

2.4. Aquifer Properties

2.4.1. Hydraulic Conductivity

Aquifer properties applicable to this model consist of hydraulic conductivity, storage, and existing concentrations of EDB distributed through the aquifer. Hydraulic conductivity is a numerical value that indicates the relative ease with which groundwater may pass through permeable geologic material. It is usually determined from aquifer tests but may also be determined qualitatively from making interpretations about depositional environments, sedimentology, and lithology. Hydraulic conductivity is the most important aquifer property for developing groundwater flow models and it directly influences simulated groundwater gradients and velocity. The following sources of information were consulted for determining model hydraulic conductivity.

- **Kirtland AFB BFF Quarterly Monitoring and Site Investigation Report, July-September (2011):** Hydraulic conductivity available from slug test analyses sheets for monitoring wells installed as part of the Kirtland AFB site investigation.

- **Kirtland AFB Stage 2 Abatement Plan, Extraction Well KAFB-ST105-EX01, Aquifer Test Report (2009):** Contains pumping test data for wells at the southern part of the model domain.

- **Source Water Assessment for the Albuquerque Water Supply System, NMED, (2002):** Hydraulic conductivity referenced to other reports including Thorn (1993) and Groundwater Management, Inc. (1988).

- **McAda and Barroll (2002), Kernoodle (1998), and other USGS reports:** Contain hydraulic conductivity data, maps, and multiplication factors for anisotropy across the Albuquerque basin.

- **Thorn and others (1993):** Hydraulic conductivity given by dividing transmissivity (T) by screen length (b) in Table 2 of the USGS report (T = Kb).

- **Hawley and Haase (1992):** Presents ranges of hydraulic conductivity with rankings of high (> 30 ft/d), moderate (0.3 to 30 ft/d) and low 0.3 ft/d. Rankings based on depositional environments and particle sizes (sand + gravel/silt + clay ratio).

- **Groundwater Management, Inc. (1988):** Hydraulic conductivity calculated for Ridgecrest Wells 1-4 from pumping tests (Table 1 of GMI report). Calculations used *best estimate* of transmissivity divided by screen length.

Pumping test results reported for ABCWUA wells are more representative of hydraulic conductivity for wider and deeper sections of the Santa Fe Group aquifer than results from KABF slug tests. This is because pumping tests account for long well screens in production wells and encompass a greater overall area of testing. On the other hand, slug testing from the Kirtland AFB site investigation has provided a greater density of hydraulic conductivity data in shallow parts of the aquifer which seems relevant to designing hydraulic controls at the source area and plume front. It is important to use correct hydraulic conductivity data for design purposes because, as pointed out by Doriski and others (1994), inaccurate estimates of hydraulic conductivity used for designing groundwater remediation systems can result in underdesign or overdesign problems creating incomplete capture of a contaminant plume, unnecessary expenditures, and other related problems.

A comparison of data from pumping and slug tests indicates the data sets are similar. However, in comparing data sets it is necessary to keep in mind the spatial differences from where each data set was collected in relation to the ancestral Rio Grande deposits. The model domain is larger than the current plume size (fig. 2) and includes ABCWUA wells and pumping test locations outside (east and west) of the ancestral Rio Grande deposits. Hydraulic conductivity results from pumping tests at wells in the model domain range from 6 to 131 ft/d with a mean of 45 ft/d. However, by excluding pumping test results from wells outside the ancestral Rio Grande deposits, results are higher on average (72 ft/d). Hydraulic conductivity from slug tests performed at monitoring wells located in the central part of the model domain within the ancestral Rio Grande deposits

range from 41 to 107 ft/d with a mean of 70.4 ft/d. Hydraulic conductivity is even higher in some areas as shown by pumping tests conducted as part of the Stage 2 Abatement Plan, Solid Waste Management Unit ST-105 at Kirtland AFB, which resulted in hydraulic conductivities of 131 and 246 ft/d (Kirtland AFB, 2009).

2.4.2. Storage

A value of 0.2 was selected for specific yield (storage term for unconfined aquifers) based on work by Bjorklund and Maxwell (1961), Thorn and others (1993), Kernodle and others (1995), McAda and Barroll (2002), and Bexfield and McAda (2003). Although some deeper layers of the Santa Fe Group aquifer may be confined, specific storage (the storage term for confined aquifers) is not used in steady-state simulations. A value of 0.274 was assigned for effective porosity based on slug tests performed during the Kirtland AFB site investigation. Kirtland AFB reported laboratory tests for porosity from remolded soil samples from well screened intervals (Kirtland AFB, 2013).   Those results showed a mean total porosity of 34.3 % with a standard deviation of $\pm$ 4.78%. Based on these and other (published) data, total porosity in the model was generally 30%, although some iterations of the model used a porosity of 35%.

2.4.3. Existing EDB Concentrations

The EDB plume can be included as distributed property data by essentially replicating the current plume at the start of a model run. Because EDB is distributed through the aquifer, it is more appropriate to include EDB as a property of the aquifer than a contaminant boundary condition. The data sources for constructing the plume in the model are reports from the Kirtland AFB site investigation. The model includes each of the three concentration depth zones which ultimately undergo mixing during the mass transport model run.

United States
Environmental Protection
Agency

2.5.   1,2-Dibromoethane Transport Processes

2.5.1.   Degradation and First-Order Decay

A cursory review of EDB concentrations from selected Kirtland AFB groundwater monitring wells for the years 2008 to 2012 did not clearly indicate a trend of decreasing concentrations. Some wells showed slight decreases but others did not. Wilson and others (2008) report that although it is theoretically possible for anaerobic biodegradation or abiotic degradation to remove EDB, it is frequently difficult to prove based on conventional monitoring data. They propose performing Compound Specific Isotopic Analysis (CSIA) as a more definitive method to determine biodegradation.

Rather than including degradation in the model, an approach more consistent with current knowledge is to develop the mass transport model without using degradation. However, since more thorough investigative work may eventually be performed on understanding degradation at the site, a contingency for including EDB degradation in the model was included. In the event additional data shows degradation is occurring, degradation can be included in the model as first-order irreversible decay. This requires a first-order reaction rate that can be estimated by the following equation:

Equation 2: First-order decay

$$\ln \frac{[A]}{[A]_0} = -kt$$

where

k	=	the reaction rate constant
$[A]_0$	=	the initial concentration
$[A]$	=	the concentration at time *t*

Wilson and others (2008) provided a summary of first-order rate constants compiled from several field studies of EDB in aquifer flow paths. For spills of leaded gasoline, the rate constants are 1.3/yr, 0.63/yr, and 0.22/yr. One rate constant is reported for a spill of AVGAS which is 0.03/yr.

2.5.2. Sorption and Retardation

Sorption refers to a number of different processes (adsorption, absorption, chemisorption, etc.) that remove a solute from solution by becoming attached or incorporated into solid material such as sediment and mineral grains. When sorption occurs it decreases contaminant concentrations and reduces the velocity of contaminant movement which is referred to as retardation.

The distribution coefficient (K_d) is the slope of a linear sorption isotherm and can be calculated by multiplying the distribution coefficient for soil organic carbon (K_{oc}) by the fraction of organic carbon (f_{oc}). Whether or not retardation is occurring can be estimated from calculating a retardation factor (r_f) as shown in equation 3.

Equation 3: Retardation factor

$$r_f = 1 + \frac{B_d}{\theta} \, K_d$$

where

r_f	=	retardation factor
B_d	=	bulk density of soil
θ	=	porosity
K_d	=	distribution coefficient ($f_{oc} \cdot K_{oc}$)

Following the calculation of r_f, the relative velocity of a solute front (plume front) can be determined by dividing the average linear velocity of groundwater by the retardation factor (equation 4).

Equation 4: Relative velocity of contamination

$$V_c = \frac{V_x}{r_f}$$

where

V_c = average linear velocity of the solute front
V_x = average linear groundwater velocity

EPA United States
Environmental Protection
Agency

This calculation has been performed by Shaw (2011) using the following values from literature and testing: K_{oc} 28.2 milliliters per gram (mL/g) (EPA, 2006), B_d 2.65 grams per cubic centimeter (g/cm^3), f_{oc} 0.00023 gram/gram, and a porosity of 34.1%. The resulting retardation factor is 1.03, and the average linear velocity of the EDB plume front is 0.97. Based on this estimate, it appears that little sorption is taking place and the plume front would be moving at nearly the same velocity as groundwater.

If more extensive site investigations indicate sorption is occurring, the model can be modified. Sorption can be included by specifying a distribution coefficient, an initial concentration, and by specifying the type of sorption isotherm (linear, Freundlich, or Langmuir; (Fetter, 2008)). Although sorption is not known to be occurring at this time, the concentration along the plume front should not be expected to be constant based on the processes of dispersion as noted below.

2.5.3. Dispersion

Dispersion is a process that spreads contaminant mass in the lateral and vertical (x, y, and z) directions, along the advective path of a plume, and reduces solute concentrations (Schlumberger, 2012). When dispersion causes solute concentrations at a plume front to be reduced, it takes a greater length of time for a given higher concentration to reach a point down gradient. Higher values of dispersion in a model cause more mixing and lower values of dispersion cause less mixing.

Dispersion consists of two components: mechanical dispersion and molecular diffusion, which together are referred to as hydrodynamic dispersion. Mechanical dispersion is caused by groundwater moving though individual flowpaths in porous media where some flowpaths cause groundwater velocities to be greater, and some less, than the average linear groundwater flow velocity. Mechanical dispersion occurring along the axis of a plume is called longitudinal dispersion, and mechanical dispersion occurring perpendicular to the axis is called transverse (or horizontal) dispersion. Molecular diffusion causes solute to move from a higher to lower concentration even

when water is not flowing. Molecular diffusion is usually insignificant for groundwater modeling purposes.

The model requires a dispersion coefficient based on values of longitudinal, horizontal, and vertical dispersivity (equation 5).

Equation 5: Dispersion coefficient
Schlumberger, 2012

$$D = \propto_L \cdot \frac{V_L^2}{|v|} + \propto_H \cdot \frac{V_H^2}{|v|} + \propto_v \cdot \frac{V_v^2}{|v|} + D*$$

where

D : Dispersion Coefficient (L^2/T)

$\propto_L$: longitudinal dispersivity (L)

V_L : longitudinal velocity of flow along the plume migration pathway (L/T)

$\propto_H$: is the horizontal dispersivity (L)

V_H : horizontal velocity of flow along the plume migration pathway (L/T)

$\propto_v$: vertical dispersivity (L)

V_V : vertical velocity of flow along the plume migration pathway

$D*$: diffusion coefficient (L^2/T)

$|v|$: magnitude of seepage velocity (L/T)

In order to determine dispersivity ($\propto$), the length of the EDB plume may be used in a relationship by Xu and Eckstein (1995) or in a method referred to as the "one-tenth rule". The Xu and Eckstein relationship is shown in equation 6.

Equation 6: Longitudinal dispersivity
Xu and Eckstein, 1995

$$\propto_m = 0.83 \, (\log L_s)^{2.414}$$

where

$\propto_m$: longitudinal dispersivity

L_s : length of plume (in meters)

EPA United States Environmental Protection Agency

If the plume length is calculated from approximately the middle of the LNAPL area to the vicinity of the Ridgecrest wells 3 and 5, the distance is approximately 10,000 ft (3,048 m).

$$\propto_m = 0.83 \ (\log \ 3{,}048 \ m)^{2.414}$$

$$\propto_m = 0.83 \ (3.48 \ )^{2.414}$$

$$\propto_m = 0.83 \ \cdot 20.35$$

$$\propto_m = 16.89 \ m = 55.4\text{ft}$$

The "one-tenth rule" refers to estimating dispersivity as being 0.1 of the length of the plume. However, the "one-tenth rule" is less appropriate to this model because, as reported by Fetter (2008), for longer plumes the relationship between longitudinal dispersivity and flow length is more complex than a 0.1 ratio. Therefore, the better estimate is believed to be the value calculated by the Xu and Eckstein equation.

In a study of field-scale dispersion in aquifers, Gelhar and others (1992) reported that horizontal values were found to be 1-2 orders of magnitude less than longitudinal values, and vertical values even smaller by still another order of magnitude. Based on this research, and on model testing, the ratios of transverse to longitudinal and vertical to longitudinal dispersivity were determined to be 0.01 and 0.001, respectively.

Molecular diffusion is not used in equation 5 because the length of the plume suggests that mechanical dispersion is the predominant cause of mixing and molecular diffusion would be negligible. Velocity values in equation 5 are calculated in the model.

EPA United States Environmental Protection Agency

3. MODEL CONSTRUCTION

3.1. Model Grid and Layers

The model uses a variably spaced finite-difference grid oriented north to south. The grid origin (at point 0,0) corresponds with coordinates 1,155,970 ft (x-direction) and 12,723,100 ft (y-direction) (North American Datum 1983). From the origin the grid extends 25,697 ft east and 20,898 ft north, and includes 178 rows and 154 columns. Sizes of grid cells range from 10, 609 ft^2 to 265,225 ft^2. A refined grid was needed for mass transport modeling and thus smaller grid cells cover the main area of interest: the EDB plume, Ridgecrest wells, VA hospital production well, etc. The model grid is shown in figure 4.
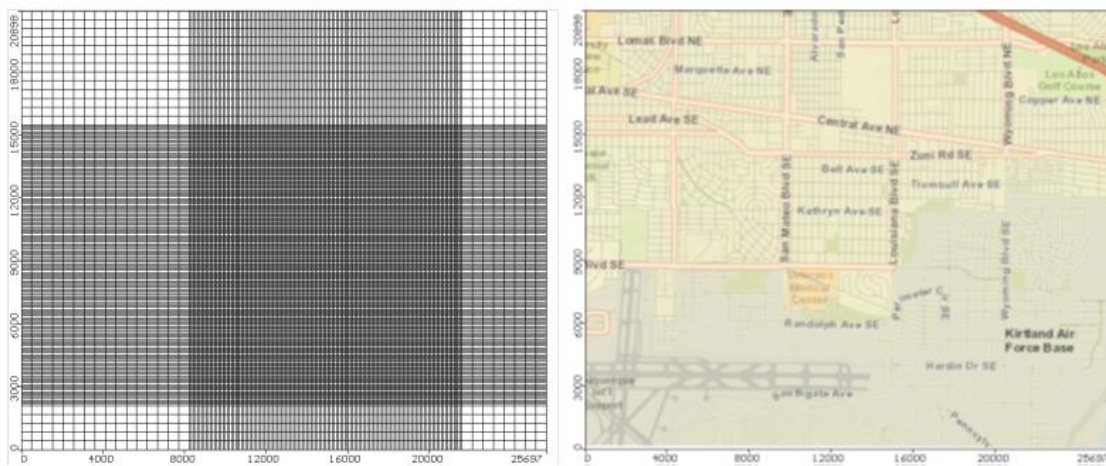
Figure 4: Model grid and model domain.
Model grid (left) shown in relation to model domain (right)

The model contains eight main layers (fig 5). Layering was determined based on the model's functional needs rather than on elevations of geologic strata. The main model layers are:

- **Layers 1 and 2:** These layers contain the water table (bottom of layer 1), and the LNAPL area (layer 2) represented as a contaminant concentration boundary.

EPA United States Environmental Protection Agency

- **Layers 3, 4, and 5:** These layers contain the EDB plume divided into the shallow interval (layer 3), intermediate interval (layer 4), and deep interval (layer 5). These three divisions are only important at the beginning of the model run because concentrations from all three layers undergo mixing when the mass transport model run begins.

- **Layers 6, 7, and 8:** Contain well screens for drinking water production wells.

In addition to the layers described above, others layers were added and/or removed on an as needed basis to define zones needed for ZoneBudget, the computer program used to calculate water volumes. Table 1 provides information on model layer elevations, thicknesses, and uses.
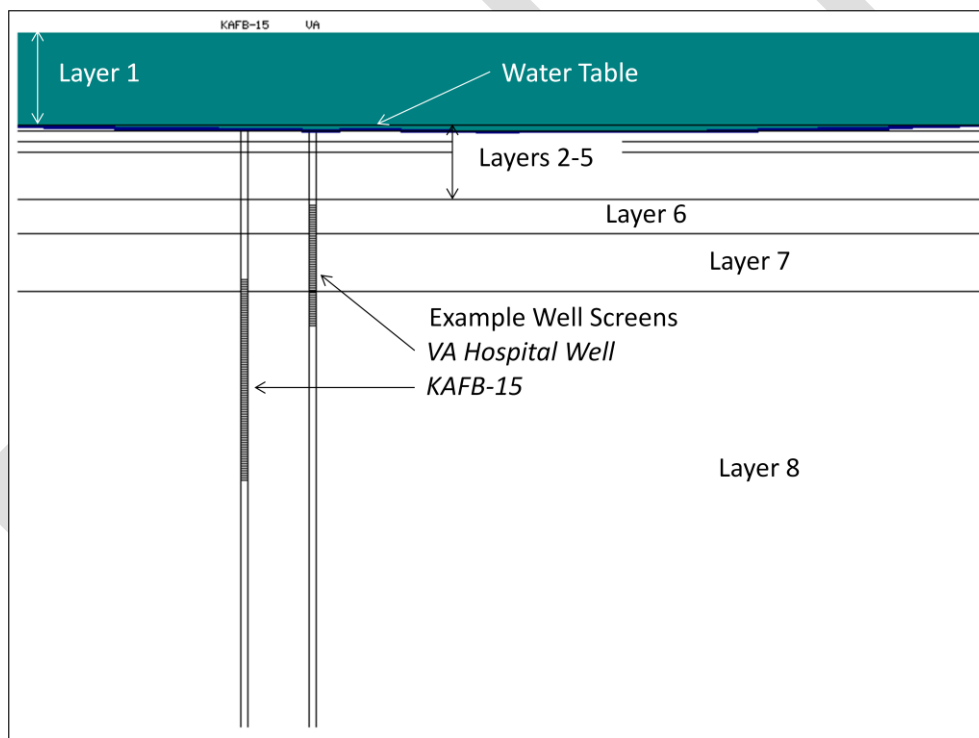
Figure 5: Model layers in cross-section.

3.2. Model Time

Groundwater flow and EDB transport use time differently in the model. Groundwater flow was developed as a steady-state condition representing pumping conditions and groundwater levels for approximately fall 2011 through winter 2012. This

time period represents the beginning of the project when model data collection and reviews of data began. Steady-state refers to groundwater conditions at equilibrium, so there are no changes to groundwater conditions in the model once the groundwater flow field has been established by MODFLOW.

Table 1: Model Layer Specifications

Model Layers	Top Elevation	Bottom Elevation	Thickness (ft)	Main Purposes
1	5000	4864	136	contains water table
2	4864	4855	9	water table; EDB source (LNAPL)
3	4855	4839	16	EDB plume shallow
4	4839	4824	15	EDB plume intermediate
5	4824	4754	70	EDB plume deep
6	4754	4703	51	production well screens
7	4703	4620	83	production well screens
8	4620	3880	740	production well screens

There are a number of reasons why groundwater flow should be steady-state and time should be based on recent conditions. First, in order to determine pumping designs to stop or limit EDB plume movement, the design analysis must use current groundwater levels for model calibration and the current known extent of EDB contamination for initial mass transport conditions. Second, groundwater level measurements from within the plume have been collected in only the last few years. These recent data are essential for ensuring MODFLOW calculates hydraulic heads accurately. Although there is a record of basin-wide changes in groundwater levels and levels appear to be rising at present, it is more practical from a design standpoint to base model development on current groundwater conditions.

Different than groundwater flow, the time for EDB transport covers 75 years beginning in 2011. *(The model was not designed to simulate movement of EDB from the time of the initial release of fuel below the BFF).* Seventy-five years was selected because it provides ample time for EDB to travel sufficiently far into the Ridgecrest well field so that effects can be examined. Seventy-five years also provides enough time for an analysis of plume capture. The seventy-five year period may be shortened or

lengthened as necessary in future model revisions, but extremely long run times such as 100s of years are not practical because of computer processing limitations.

3.3. Boundary Conditions

3.3.1. Hydraulic Boundaries

Specified head boundaries were used around the north, south, east, and west edges of the model domain in all layers. Each side was divided into two individual boundary segments so there are eight groundwater flow boundaries in all. Using eight segments helped provide flexibility for flow calibration. The boundaries were assigned with lateral gradients to account for changes in head along boundary lengths. The cone of depression beneath southeast Albuquerque, intersecting horizontal flow boundaries, causes head values to gradually change from relatively higher values at the ends of each boundary to relatively lower values towards the center.

Boundary values and gradients were refined during model development to improve flow calibration. Boundaries were refined by adjusting hydraulic head, boundary conductance, and lengths of individual boundary segments to improve consistency between calculated and observed water levels. According to the approved QA/QC project plan, successful head calibration refers to achieving 10% or less for the normalized root mean square for observed vs. calculated heads. While making adjustments to flow boundaries, it was noticed that there is not a unique set of boundary conditions resulting in successful head calibration. In other words, a range of possible boundary heads and gradients can provide acceptable calibration. This range of possibilities indicated a sensitivity analysis was warranted on flow boundary specifications and is discussed fully in Chapter 5.

3.3.2. EDB Source Boundary

The area referred to as the LNAPL area in the conceptual model was treated as a contaminant concentration boundary. The purpose of this boundary is to provide concentrations of EDB to the dissolved phase plume. The boundary was placed in layer 2 just above the shallow zone in layer 3 (fig 6), and reflects EDB concentrations in 2011.

The most important attributes about the boundary are its horizontal extents, its starting concentration, and its rate of concentration decrease. The thickness of the boundary is not important because the boundary thickness does not affect the transfer of EDB to the underlying shallow zone.

The boundary's starting concentration was assumed to be similar to higher concentrations of EDB reported for the shallow zone during the 4th quarter of 2011. The highest concentration listed in the shallow zone is 190 µg/l (Shaw Environmental and Infrastructure, Inc., 2011), and the boundary concentration was set at 200 µg/l for convenience. The boundary undergoes a decrease in concentration of 10% per year. This decrease not based on sampling data and is explained further in the uncertainties section (Section 5.1).
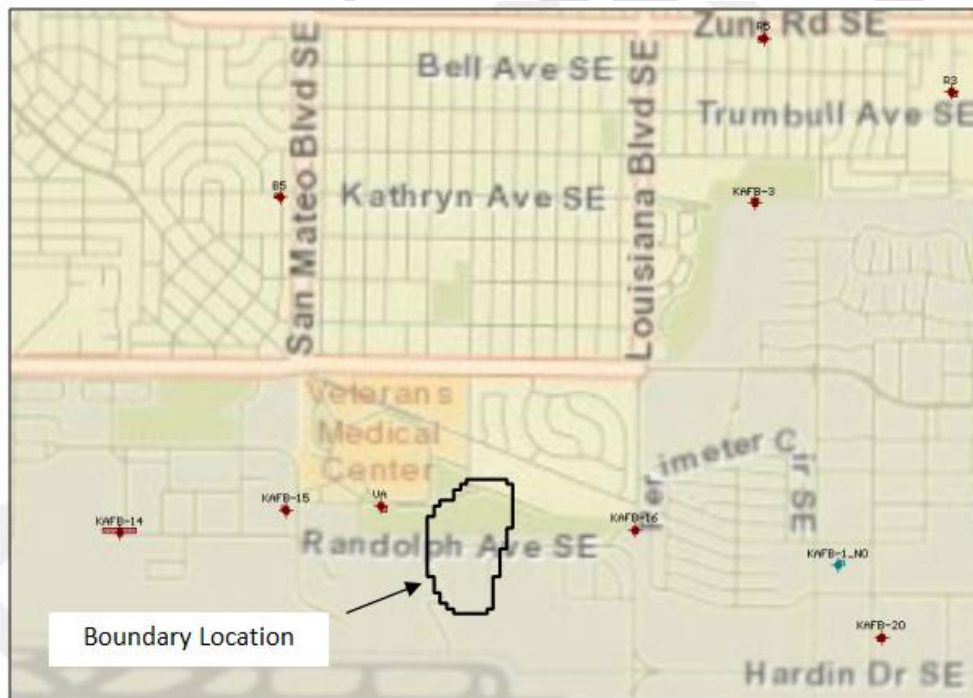
Figure 6: Contaminant concentration boundary.

3.4. Drinking Water Production Wells

The production of groundwater from the Santa Fe Group aquifer system is the single most important factor affecting groundwater flow directions in the model domain.

The model contains nineteen active drinking water production wells operated by ABCWUA (12 wells), KAFB (6 wells), and the VA (1 well). These wells are represented in the model by their coordinate locations, pumping rates, and elevations of the tops and bottoms of their well screens. Figure 7 shows locations of drinking water production wells.

Figure 7: Locations of pumping wells in model domain.

Production wells identified on maps, but were either temporarily inactive or had been permanently removed from service during the groundwater flow simulation period, were not included. Those wells are KAFB-1, KAFB-2, KAFB-5, KAFB-6, KAFB-12, KAFB-13, and Love-5. One other well, KAFB-4, is an active production well but was not included because it lies too close to the southern model boundary. A pumping well placed close to a flow boundary may cause anomalous flow conditions and KAFB-4 was therefore not included.

EPA United States Environmental Protection Agency

Well location coordinates and screen elevations for ABCWUA wells were taken from a listing of well construction information and summary statistics found in Bexfield and others (1999). Ridgecrest wells 1-4 were imported into the model according to their geographic coordinates. Once imported, their locations were checked by comparing the model plot to a detailed area map found in Groundwater Management Inc. (1988). Since Ridgecrest 5 was installed after 1988 (in 1991) its location was noted during a May 2012 site reconnaissance trip and later plotted in the model accordingly. Locations of other ABCWUA wells in the model were taken from various published reports such as Bexfield and McAda (2003).

The Kirtland AFB Environmental Restoration Program provided a base-wide map showing locations of all base production wells. The New Mexico Veterans Affairs Health Care System, Engineering Services, provided geographic coordinates for the VA hospital production well. All wells in the model (both production and monitoring wells) were compared to well locations shown on various maps in Kirtland AFB site investigation reports and other reports to ensure location accuracy and consistency.

Pumping rates for city wells were provided by ABCWUA and pumping rates for Kirtland AFB wells were provided by the Kirtland AFB Environmental Restoration Program. ABCWUA and the VA provided pumping rates for February 2012, and Kirtland AFB provided data for May 2012. In looking at trends in Kirtland AFB production rates, winter rates can be as much as 50% less than spring and summer rates. Therefore, to approximate winter pumping rates for steady-state model time, 50% of the Kirtland AFB May 2012 pumping rates were used.

The model requires specific information for each pumping well, including a well name, well location coordinates, the top and bottom well screen elevations, and pumping rates. This information is contained in table 2. Well screens that cross model layers pump water from each model layer. Pumping rates are listed with a negative sign (-) to indicate water extraction. NMED has notified EPA that Ridgecrest 5 usually pumps more than Ridgecrest 3. The effects of this difference from the pumping rates below were evaluated during the sensitivity analysis (Chapter 5).

3.5. Aquifer Properties

3.5.1. Hydraulic Conductivity and Storage

Hydraulic conductivity was established in consultation with NMED. Data used to establish the field hydraulic conductivity is listed in table 3, and consists of pumping test data reported for drinking water supply wells. Slug test results were not used because pumping tests are more comprehensive in nature, although results from both types of tests are similar in this case.

Table 2: Pumping well coordinates, well screen elevations, and pumping rates.

Well Name	Model Designation	X Coordinate	Y Coordinate	Screen Top (ft msl)	Screen Bottom (ft msl)	Screen Length (ft)	Pumping Rate (gpm)
Burton-1	B1	1159778	12734836	4646	4030	616	-3000
Burton-2	B2	1160894	12737042	4857	4437	420	-2300
Burton-3	B3	1161920	12738845	4857	4221	636	-1900
Burton-4	B4	1158921	12733232	4645	4000	645	-2850
Burton-5	B5	1165506	12734339	4728	4128	600	-2850
Love-3	LOVE_3	1180335	12741892	4805	4145	660	-1500
Love-4	LOVE_4	1177095	12741942	4770	4086	684	-1700
Ridgecrest-1	R1	1180148	12735121	4806	4182	624	-1550
Ridgecrest-2	R2	1178848	12737062	4686	3916	770	-3000
Ridgecrest-3	R3	1175921	12735894	4765	3949	816	-2770
Ridgecrest-4	R4	1173480	12739269	4772	3932	840	-2800
Ridgecrest-5	R5	1173025	12736748	4705	3905	800	-2900
KAFB-3	KAFB-3	1172863	12734202	4912	4462	450	-325*
KAFB-7	KAFB-7	1170864	12725606	4904	4395	509	-391*
KAFB-14	KAFB-14	1162962	12729168	4950	4330	620	-733*
KAFB-15	KAFB-15	1165545	12729496	4642	4346	296	-840*
KAFB-16	KAFB-16	1170967	12729154	4904	4395	509	-725*
KAFB-20	KAFB-20	1174792	12727450	4904	4395	509	-767*
VA Well	VA	1167026	12729543	4751	4571	180	-760

*50% of summer pumping rate

Pumping test data were interpolated by kriging (fig 8). Two control points needed to be added to the lower southeast edge of the model domain to constrain irregular contour lines in that portion of the domain. This improved consistency between the pattern of contoured data and the general north-south pattern of hydraulic conductivity expected in this geologic setting. Aquifer storage was assigned as reported in Section 2.4.2 throughout the model domain.

Table 3: Hydraulic conductivity (K) in x, y, and z directions.
Data for wells outside the model domain were also used in contouring.

Well	K_x, K_y	K_z
Burton-2	50	5.00
Burton-3	40	4.00
Ridgecrest-1	13	1.30
Ridgecrest-2	25	2.50
Ridgecrest-3	24	2.40
Ridgecrest-4	25	2.50
Ridgecrest-5	80	8.00
LOMAS-1	28	2.80
LOVE-6	6	0.60
LOVE-1	12	1.20
LOVE-7	23	2.30
LOVE-3	47	4.7
LOVE-4	35	3.5
LOVE-5	25	2.5
LOVE-8	71	7.10
CHARLES-4	98	9.8
CHARLES-2	100	10.0
CHARLES-5	57	5.7
CHARLES-3	120	1.20
CHARLES-1	103	1.03
SANTA_BARBARA	34	3.4
YALE-1	24	2.40
YALE-2	2	2.40
YALE-3	12	1.20
SAN_JOSE-2	8	0.8
MILES-1	13	1.30
KAFB-ST105-EX1	131	1.31
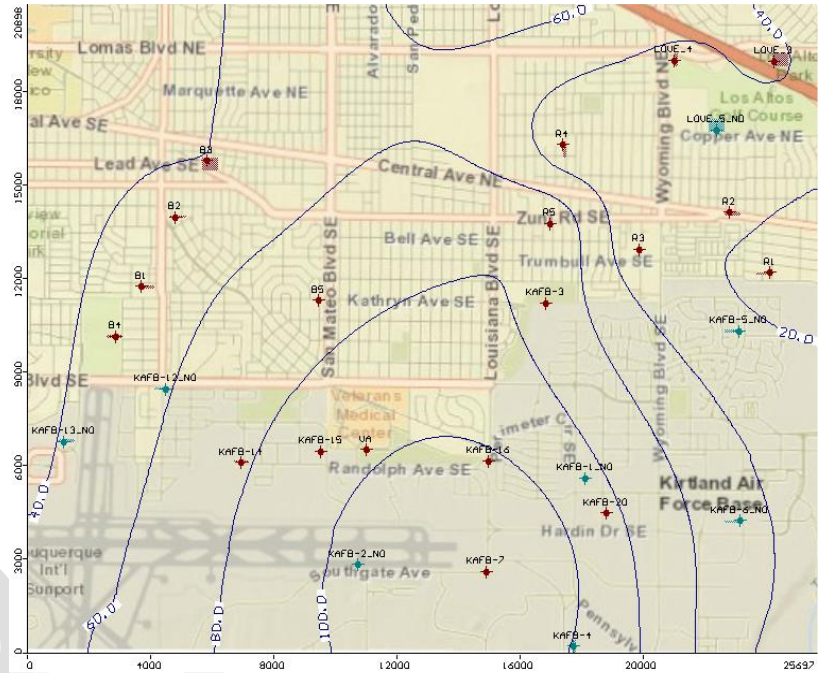
Figure 8: Contoured field of hydraulic conductivity.

3.5.2. EDB Plume Concentrations

The existing EDB plume was included as an aquifer property by assigning EDB concentrations from the 4th quarter 2011 to layers 3, 4, and 5 using data from Kirtland AFB site investigation (tables 4-6). These three property zones were combined with the contaminant boundary condition representing LNAPL to arrange the model's starting conditions at time 0-days (fig 9).

EPA United States Environmental Protection Agency
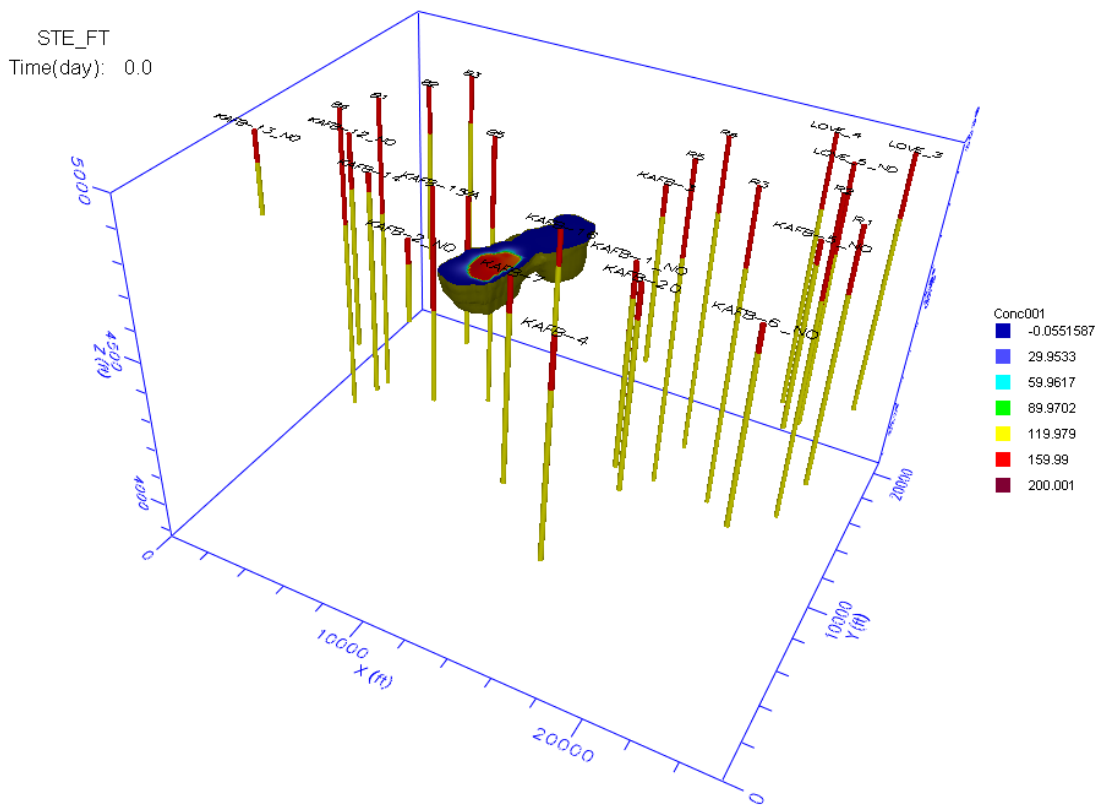
Figure 9: Initial conditions for EDB in 3-dimensional diagram.
Wells shown by red and yellow vertical lines (well screens are yellow, and red lengths are non-screened sections). Concentrations in µg/l.

3.6. Dispersion and Molecular Diffusion

The only contaminant transport process specified in the model at this time is dispersion. Dispersion was included as discussed in Section 2.5.3, and molecular diffusion was not used. Although sorption and retardation are also not included, they could be used in future versions of the model, if necessary.

Table 4: Starting concentrations for EDB in shallow zone (layer 3).

Well ID	X	Y	µg/l
KAFB-106029	1168438	12732178	0.028
KAFB-106032	1167637	12731297	0.028
KAFB-106035	1169684	12731525	0.43
KAFB-106038	1169405	12730177	0.029
KAFB-106042	1169697	12733054	0.65
KAFB-106046	1168844	12728704	0.029
KAFB-106049	1168767	12732782	0.028
KAFB-106051	1168769	12732827	0.028
KAFB-106052	1169097	12732765	0.029
KAFB-106055	1169812	12732389	0.65
KAFB-106057	1169841	12732388	0.77
KAFB-106059	1167731	12728796	190
KAFB-106064	1168370	12728893	5.3
KAFB-106067	1168764	12729817	0.097
KAFB-106075	1168230	12730338	0.21
KAFB-106076	1167813	12728331	110
KAFB-106079	1168267	12729184	160
KAFB-106085	1168603	12731085	0.039
KAFB-106088	1169265	12730858	0.26
KAFB-106091	1169060	12731912	0.028
KAFB-106094	1168133	12729819	2.3
KAFB-106106	1169420	12732797	0.2
KAFB-1061	1167369	12728699	0.32
KAFB-10610	1168474	12729865	130
KAFB-10611	1168827	12729119	0.029
KAFB-10612	1167504	12729156	0.028
KAFB-10613	1167704	12729849	0.028
KAFB-10614	1168428	12729122	57
KAFB-10615	1171267	12731530	0.028
KAFB-10616	1166990	12728286	0.028
KAFB-10617	1168953	12730327	0.6
KAFB-10618	1168458	12730534	0.6
KAFB-10619	1168998	12729810	0.34
KAFB-1062	1167064	12729130	0.028
KAFB-10620	1167900	12730479	0.028
KAFB-10621	1168427	12731187	0.15

EPA United States Environmental Protection Agency

KAFB-10622	1169410	12731591	0.9
KAFB-10623	1169743	12730758	0.029
KAFB-10624	1167595	12728634	0.028
KAFB-10625	1169030	12732396	0.18
KAFB-10626	1169857	12733703	0.029
KAFB-10627	1167436	12727518	0.029
KAFB-10628-510	1168347	12729436	8.4
KAFB-1063	1166432	12729146	0.028
KAFB-1064	1167057	12729479	0.028
KAFB-1065	1167915	12729109	64
KAFB-1066	1168163	12728404	1.4
KAFB-1067	1168340	12728000	0.028
KAFB-1068	1168188	12728778	0.8
KAFB-1069	1167968	12729234	1.1
KAFB-3411	1167787	12729001	0.028

Table 5: Starting concentrations for EDB in intermediate zone (layer 4).

Well ID	X	Y	µg/l
KAFB-106036	1169706	12731524	0.28
KAFB-106039	1169420	12730163	0.028
KAFB-106044	1167441	12727488	0.029
KAFB-106047	1168788	12728701	0.028
KAFB-106063	1168382	12728868	0.028
KAFB-106077	1167794	12728315	0.021
KAFB-106080	1168231	12729137	0.25
KAFB-106057	1169841	12732388	0.77
KAFB-106050	1168769	12732861	0.028
KAFB-106053	1169098	12732796	0.028
KAFB-106030	1168440	12732207	0.028
KAFB-106033	1167603	12731297	0.029
KAFB-106060	1167753	12728774	0.028
KAFB-106065	1168305	12729430	0.028
KAFB-106069	1168742	12729800	0.22
KAFB-106072	1168928	12731007	1.1
KAFB-106073	1168222	12730368	0.053
KAFB-106083	1168556	12730443	0.69
KAFB-106086	1168590	12731071	0.55
KAFB-106089	1169258	12730889	0.33
KAFB-106092	1169091	12731894	0.15
KAFB-106095	1168118	12729843	0.037
KAFB-106097	1167729	12729847	0.029
KAFB-106099	1167033	12729473	0.029
KAFB-106103	1169720	12730773	0.029
KAFB-106105	1169418	12732762	0.077

United States
Environmental Protection
Agency

Table 6: Starting concentrations for EDB in deep zone (layer 5).

Well ID	X	Y	µg/l
KAFB-106037	1169662	12731526	0.24
KAFB-106048	1168813	12728720	0.029
KAFB-106062	1168396	12728894	0.028
KAFB-106058	1169873	12732378	0.57
KAFB-106043	1169679	12733040	0.029
KAFB-106054	1169101	12732875	0.029
KAFB-106034	1167621	12731266	0.029
KAFB-106031	1168441	12732236	0.028
KAFB-106061	1167768	12728795	0.029
KAFB-106045	1167412	12727517	0.029
KAFB-106071	1168932	12730932	0.028
KAFB-106081	1168205	12729184	0.029
KAFB-106066	1168348	12729480	0.028
KAFB-106040	1169399	12730157	0.028
KAFB-106074	1168199	12730350	0.028
KAFB-106087	1168590	12731104	0.028
KAFB-106090	1169253	12730917	0.029
KAFB-106093	1169091	12731924	0.028
KAFB-106098	1167726	12729876	0.029
KAFB-106100	1167046	12729448	0.028
KAFB-106102	1166417	12729168	0.029
KAFB-106104	1169697	12730791	0.029
KAFB-106107	1169438	12732772	0.029

3.7. Hydraulic Head Calibration Wells

Kirtland AFB site investigation reports were thoroughly reviewed to identify groundwater monitoring wells having head measurement data corresponding to the time-frame used for the groundwater flow model (fall 2011-winter 2012). Only one head measurement per well was needed because the flow model is steady-state.   Table 7 presents the data set used to calibrate the groundwater flow model.

Table 7: Hydraulic head calibration data.

Well ID	X	Y	Head (ft msl)
KAFB-0118	1165752.45	12725765.1	4860.09
KAFB-0119	1166525.42	12725760.4	4859.5
KAFB-0121	1166873.09	12725424.9	4857.14
KAFB-106029	1168439.17	12732155.7	4854.45
KAFB-106030	1168440.97	12732184.9	4854.39
KAFB-106031	1168441.8	12732213.6	4854.35
KAFB-106032	1167637.76	12731274.5	4855.19
KAFB-106033	1167604.25	12731274.5	4855.26
KAFB-106034	1167621.53	12731243.5	4855.23
KAFB-106042	1169697.92	12733031.1	4853.13
KAFB-106043	1169679.91	12733017.7	4853.27
KAFB-106044	1167442.02	12727465.6	4858.88
KAFB-106045	1167412.49	12727494.7	4858.8
KAFB-106046	1168845.12	12728681.5	4857.14
KAFB-106047	1168788.59	12728678.9	4856.98
KAFB-106048	1168814.18	12728697	4857.08
KAFB-106049	1168768.1	12732759.7	4853.52
KAFB-106050	1168770.04	12732838.8	4853.76
KAFB-106051	1168769.35	12732804.2	4853.8
KAFB-106053	1169098.96	12732773.8	4853.4
KAFB-106054	1169101.34	12732851.9	4853.38
KAFB-106055	1169812.64	12732366.4	4853.58
KAFB-106057	1169841.81	12732365	4853.62
KAFB-106058	1169873.88	12732355.2	4853.64
KAFB-106059	1167731.45	12728773.7	4856.84
KAFB-106060	1167753.54	12728751.4	4857.24
KAFB-106061	1167769	12728771.9	4857.78
KAFB-106062	1168396.77	12728870.9	4857.45
KAFB-106063	1168382.72	12728845.8	4857.27

Well ID	X	Y	Head (ft msl)
KAFB-1061	1167769	12728771.9	4857.92
KAFB-10610	1168475.01	12729842	4856.15
KAFB-10611	1168827.57	12729096.1	4856.67
KAFB-10612	1167504.56	12729133	4856.53
KAFB-10613	1167705.24	12729826	4856.52
KAFB-10614	1168428.63	12729099.1	4856.78
KAFB-10615	1171267.52	12731507.3	4854.12
KAFB-10616	1166991.03	12728263.1	4858.19
KAFB-10617	1168953.43	12730304	4855.4
KAFB-10618	1168458.4	12730511.6	4855.61
KAFB-10619	1168998.83	12729787.2	4855.58
KAFB-1062	1168396.77	12728870.9	4857.81
KAFB-10620	1167900.9	12730456.8	4855.65
KAFB-10621	1168427.86	12731164.2	4855.21
KAFB-10622	1169410.86	12731568.2	4854.25
KAFB-10623	1169743.7	12730735.1	4854.94
KAFB-10624	1167596.08	12728611.7	4857.13
KAFB-10625	1169031.02	12732373.4	4853.81
KAFB-10626	1169857.48	12733680	4852.55
KAFB-10627	1167437.03	12727495	4858.54
KAFB-1063	1168382.72	12728845.8	4858.24
KAFB-1064	1168370.56	12728870.7	4857.29
KAFB-1065	1168306.16	12729407.6	4856.86
KAFB-1066	1168348.38	12729457.8	4856.99
KAFB-1067	1168764.89	12729794.6	4857.17
KAFB-1068	1168741.05	12729804.4	4856.84
KAFB-1069	1168743.03	12729777.7	4856.57
KAFB-106201	1172676.28	12734008.2	No Data
KAFB-106204	1170759.25	12733929.2	No Data
KAFB-106207	1172093.15	12735115.5	No Data
KAFB-0524	1168135.368	12725689.76	4855.98
KAFB-10628	1168348.133	12729413.28	4856.3
KAFB-106035	1169684.809	12731502.63	4845.11
KAFB-106036	1169706.794	12731501.35	4854.36
KAFB-106037	1169662.825	12731503.9	4854.29
KAFB-106038	1169405.901	12730154.1	4855.51
KAFB-106039	1169420.736	12730140.91	4855.4
KAFB-106040	1169399.651	12730134.17	4854.4
KAFB-106052	1169097.929	12732742.52	4853.53
KAFB-106064	1168370.563	12728870.71	4856.85
KAFB-106065	1168306.16	12729407.56	4856.49
KAFB-106066	1168348.38	12729457.75	4856.59
KAFB-106067	1168764.891	12729794.59	4855.83

Well ID	X	Y	Head (ft msl)
KAFB-106068	1168741.054	12729804.44	4855.71
KAFB-106069	1168743.028	12729777.67	4855.97
KAFB-106070	1168929.334	12731017.64	4854.49
KAFB-106071	1168932.965	12730909.21	4854.93
KAFB-106072	1168929.072	12730983.98	4853.87
KAFB-106073	1168223.083	12730345.48	4855.59
KAFB-106074	1168199.711	12730327.76	4856.16
KAFB-106075	1168231.274	12730315.21	4856.1
KAFB-106076	1167813.39	12728308.09	4856.97
KAFB-106077	1167794.992	12728292.3	4856.6
KAFB-106078	1167779.952	12728307.52	4856.23
KAFB-106079	1168268.189	12729161.77	4856.86
KAFB-106080	1168232.241	12729114.1	4856.97
KAFB-106081	1168206.007	12729160.98	4856.87
KAFB-106082	1168602.531	12730413.21	4855.54
KAFB-106083	1168557.183	12730420.67	4855.53
KAFB-106084	1168589.784	12730437.43	4855.69
KAFB-106085	1168603.545	12731062.19	4854.92
KAFB-106086	1168590.927	12731048.79	4855.14
KAFB-106087	1168590.718	12731081.6	4855.19
KAFB-106088	1169265.382	12730834.97	4854.6
KAFB-106089	1169258.338	12730866.59	4854.42
KAFB-106090	1169253.468	12730894.56	4854.92
KAFB-106091	1169060.447	12731889.69	4854
KAFB-106092	1169091.465	12731871.12	4854.19
KAFB-106093	1169092.173	12731901.25	4854.13
KAFB-106094	1168133.748	12729796.26	4856.67
KAFB-106095	1168119.115	12729820.83	4856.46
KAFB-106096	1168103.898	12729793.92	4856.75
KAFB-106097	1167730.031	12729824.41	4856.4
KAFB-106098	1167726.971	12729853.92	4856.35
KAFB-106099	1167033.802	12729450.81	4857.44
KAFB-106100	1167046.681	12729425.17	4857.4
KAFB-106101	1166448.009	12729143.66	4858.07
KAFB-106102	1166417.307	12729145.19	4857.87
KAFB-106103	1169720.846	12730750.78	4854.47
KAFB-106104	1169698.051	12730768.77	4854.58
KAFB-106105	1169418.302	12732739	4852.97
KAFB-106106	1169420.74	12732773.97	4852.91
KAFB-0118	1165752.45	12725765.1	4860.09

EPA United States Environmental Protection Agency

4. MODEL OUTPUT AND RESULTS

Model construction led to the development of individual model runs which were tailored to the requirements for meeting specific project goals. A model run is simply the activation of MODFLOW, Modpath, Zone Budget, or MT3DMS to compute hydraulic heads, particle pathlines, water balances, and contaminant concentrations depending on what the project goals require. While still other specific model runs could be developed, the ones below are consistent with what was necessary to meet requested project goals described in Section 1.3

4.1. Groundwater Flow (MODFLOW)

4.1.1. Head Calibration

The basic groundwater flow field calculated by MODFLOW is provided in figure 10. This simulated groundwater flow is used for basing more complex project goals involving mass transport and hydraulic controls. Thus, it is important that simulated groundwater levels closely match actual groundwater levels measured in monitoring wells, referred to as head calibration.

Calibration goals are specified in the project QA/QC plan. The main statistic used for evaluating head calibration is the normalized root mean squared (RMS). Many groundwater modelers utilize a normalized RMS of 10% or less to indicate successful head calibration. The normalized RMS for the simulated heads in figure 10 is 6.80%. A plot of calculated vs. measured (observed) heads is shown in figure 11.

Other perspectives on calibration are given by calibration residuals and the correlation coefficient. A calibration residual is the difference between calculated heads and measured heads (table 8, found at end of Section 4.1). The distribution of residuals should ideally resemble a normal distribution with most residuals clustered around the value of zero. The mean residual for this model is -0.0195 ft. The correlation coefficient is a value indicting whether data sets for calculated and measured heads are related, and would be shown by a value relatively close to either 1.0 or -1.0. The correlation coefficient for this model simulation is 0.951.
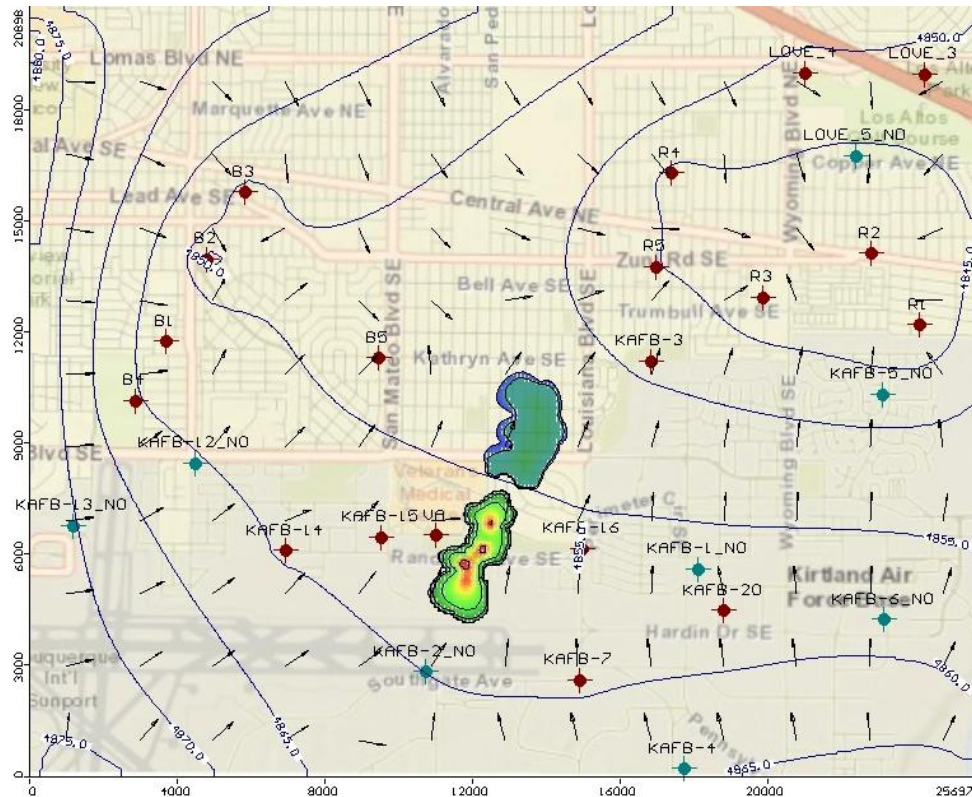
Figure 10: Map of calculated groundwater flow directions.
Map shows flow vectors/arrows, the contoured equipotential surface, and EDB at
starting concentrations (all in model layer 3).

4.1.2. Volumetric flow (Zone Budget)

The total amount of water entering the model during the flow simulation is
7,170,791.0 ft^3/d, and the total amount of water exiting is 7,172,399.0 ft^3/d. The amount
of water removed by pumping wells is 6,415,911.5 ft^3/d. Approximately 20,000 ft^3/d of
water moves from the plume front towards the Ridgecrest well field, and approximately
2,500 ft^3/d of water moves downward from the base of the EDB plume and LNAPL
source boundary to lower model layers.
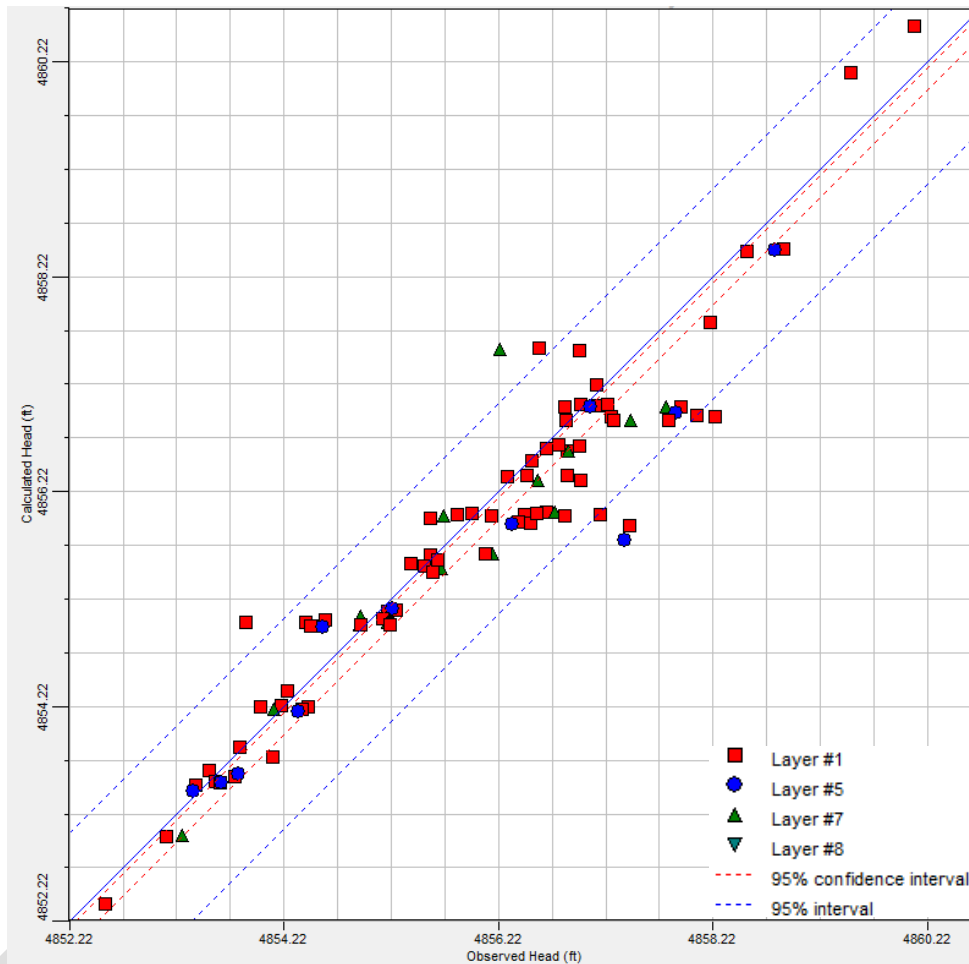
Figure 11: Calculated vs. observed heads.

4.1.3. Particle Tracking and Groundwater Velocity (Modpath)

Particle tracking was used to examine potential groundwater flow paths from the EDB plume front towards the Ridgecrest well field, and then from the western side of the plume towards the VA well. Particle tracking path lines show the movement of hypothetical water particles placed in the aquifer. They do not simulate the movement of EDB concentrations which is more complex.

Particle tracking shows different groundwater flow directions occurring at different elevations in the aquifer. This is important because the EDB plume is, for now,

United States
Environmental Protection
Agency

shallower than most water production well screens. For example, in model layer 8, particles placed below the EDB plume front are captured by Ridgecrest-5 (fig 12); while particles placed above in model layer 3 were nearly all captured by Ridgecrest-3 (fig 13). Calculated particle travel times from the EDB plume front to drinking water supply wells vary according to where each particle is initially placed. In layer 8, travel time to Ridgecrest-5 ranges from 20 years for a particle placed near the center (and below) the plume front, to 25 and 26 years for particles placed to the southeast and northwest below the plume front. For particles placed in layer 3 near the northwest part of the plume, the travel time to Ridgecrest-5 well screen is 30 years, and travel time for particles placed to the southwest and reaching Ridgecrest-3 is 70 years. Generally speaking, simulated horizontal groundwater velocity in the EDB plume vicinity ranges from approximately 0.1 ft/d to 0.6 ft/d , with higher velocities near production wells screens.

For the VA hospital production well, particles placed in model layer 3 along the western margin of the plume traveled to the VA well in 3-5 years (fig 14). This includes vertical transport from layer 3 to layers 6-8 where the well is screened.
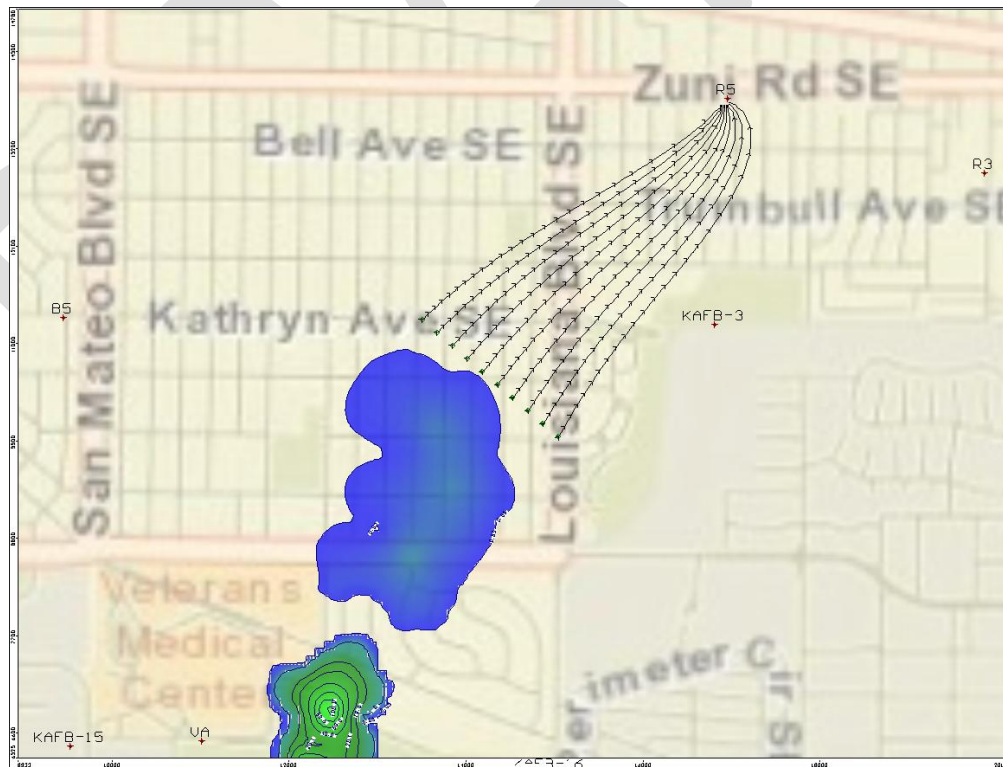

Figure 12: Particle pathlines in layer 8.
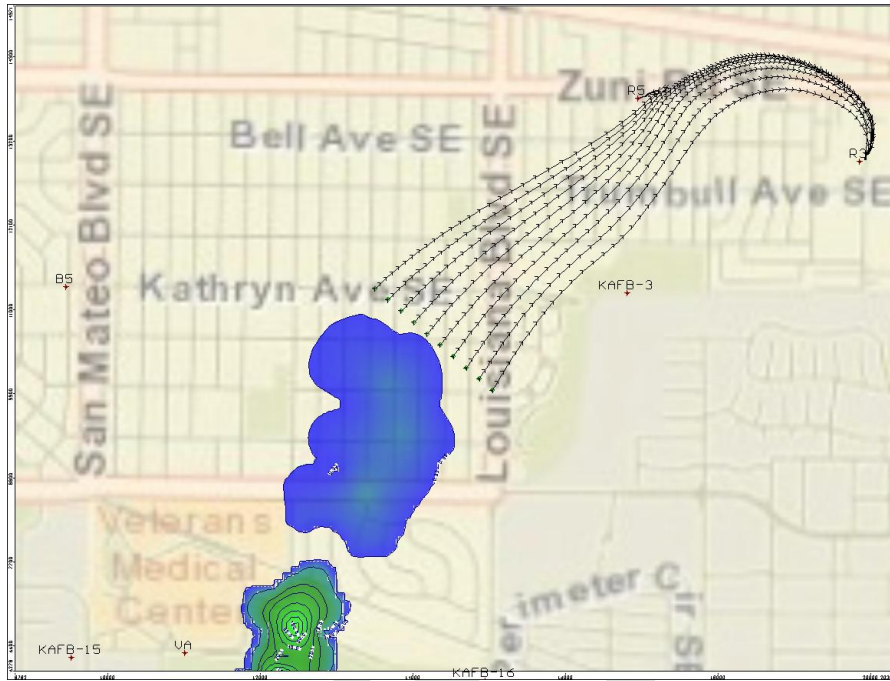Time markers on pathlines are at 1-year intervals.
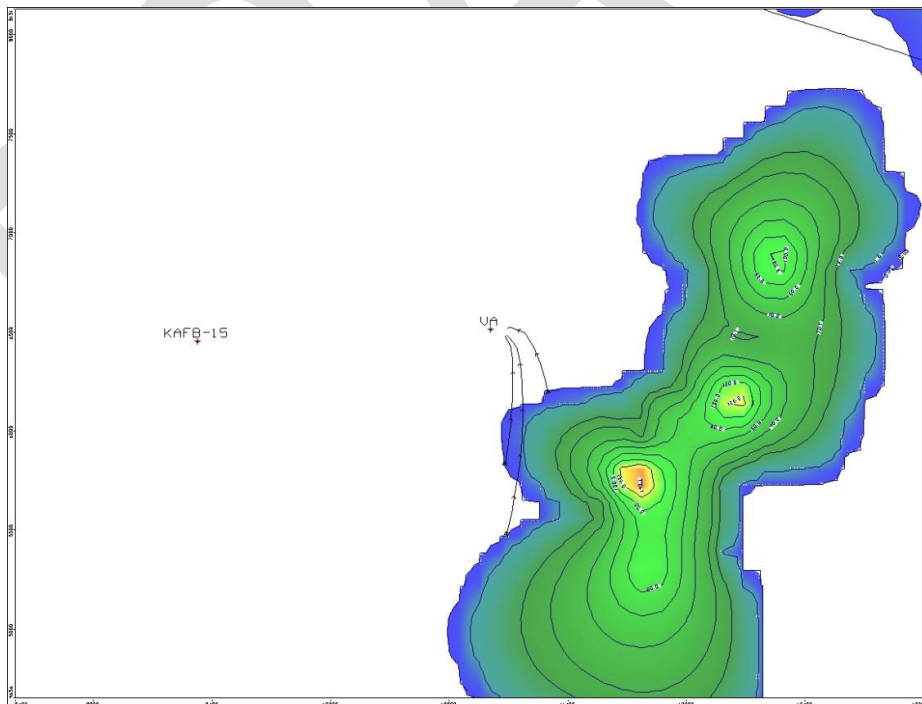
Figure 13: Particle pathlines in model layer 3.

Figure 14: Particle movement towards the VA hospital production well.

EPA United States Environmental Protection Agency

Table 8: Calibration residuals.
(Residual = Calculated - Observed)

Well Name	Calc. (ft)	Obs. (ft)	Residual (ft)
KAFB-0118/1	4860.546	4860.09	0.456387
KAFB-0119/1	4860.12	4859.5	0.620117
KAFB-106029/1	4854.213	4854.45	-0.23711
KAFB-106030/1	4854.189	4854.39	-0.20055
KAFB-106031/1	4854.167	4854.35	-0.1835
KAFB-106032/1	4855.104	4855.19	-0.086
KAFB-106033/1	4855.113	4855.26	-0.14672
KAFB-106034/1	4855.13	4855.23	-0.09963
KAFB-106042/1	4853.008	4853.13	-0.12219
KAFB-106043/1	4853.027	4853.27	-0.24266
KAFB-106044/1	4858.48	4858.88	-0.40002
KAFB-106045/1	4858.462	4858.8	-0.33809
KAFB-106046/1	4857.015	4857.14	-0.12486
KAFB-106047/1	4857.027	4856.98	0.046855
KAFB-106048/1	4857.006	4857.08	-0.07414
KAFB-106049/1	4853.631	4853.52	0.110859
KAFB-106050/1	4853.57	4853.76	-0.19018
KAFB-106051/1	4853.596	4853.8	-0.20381
KAFB-106053/1	4853.49	4853.4	0.090234
KAFB-106054/1	4853.427	4853.38	0.047246
KAFB-106055/1	4853.526	4853.58	-0.05363
KAFB-106057/1	4853.515	4853.62	-0.10535
KAFB-106058/1	4853.509	4853.64	-0.13072
KAFB-106059/1	4857.003	4856.84	0.163418
KAFB-106060/1	4857.03	4857.24	-0.20973
KAFB-106061/1	4857.006	4857.78	-0.77365
KAFB-106062/1	4856.887	4857.45	-0.56328
KAFB-106063/1	4856.912	4857.27	-0.35838
KAFB-106064/1	4856.887	4856.85	0.037207
KAFB-106065/1	4856.369	4856.49	-0.12086
KAFB-106066/1	4856.326	4856.59	-0.26432
KAFB-106067/1	4856.004	4855.83	0.174395

EPA United States Environmental Protection Agency

KAFB-106068/1	4856	4855.71	0.29
KAFB-106069/1	4856.022	4855.97	0.051973
KAFB-106070/1	4854.973	4854.49	0.482656
KAFB-106071/1	4855.06	4854.93	0.12957
KAFB-106072/1	4855	4853.87	1.13
KAFB-106073/1	4855.626	4855.59	0.035977
KAFB-106074/1	4855.642	4856.16	-0.51791
KAFB-106075/1	4855.647	4856.1	-0.45303
KAFB-106076/1	4857.534	4856.97	0.56418
KAFB-106077/1	4857.555	4856.6	0.954688
KAFB-106078/1	4857.541	4856.23	1.311016
KAFB-106079/1	4856.601	4856.86	-0.25941
KAFB-106080/1	4856.647	4856.97	-0.32254
KAFB-106081/1	4856.601	4856.87	-0.26893
KAFB-106082/1	4855.525	4855.54	-0.0151
KAFB-106083/1	4855.527	4855.53	-0.00314
KAFB-106084/1	4855.509	4855.69	-0.18072
KAFB-106086/1	4855.034	4855.14	-0.10582
KAFB-106087/1	4855.009	4855.19	-0.18072
KAFB-106088/1	4855.032	4854.6	0.431738
KAFB-106089/1	4855.007	4854.42	0.587324
KAFB-106090/1	4854.985	4854.92	0.065352
KAFB-106091/1	4854.221	4854	0.221191
KAFB-106092/1	4854.226	4854.19	0.035586
KAFB-106093/1	4854.2	4854.13	0.070195
KAFB-106094/1	4856.027	4856.67	-0.64266
KAFB-106095/1	4856.007	4856.46	-0.45268
KAFB-106096/1	4856.028	4856.75	-0.72168
KAFB-106097/1	4855.933	4856.4	-0.46738
KAFB-106098/1	4855.914	4856.35	-0.43643
KAFB-106099/1	4855.898	4857.44	-1.54156
KAFB-1061/1	4857.006	4857.92	-0.91414
KAFB-10610/1	4855.993	4856.15	-0.15684
KAFB-106100/1	4855.77	4857.4	-1.62998
KAFB-106101/1	4856.926	4858.07	-1.14422
KAFB-106102/1	4856.948	4857.87	-0.92225
KAFB-106103/1	4854.969	4854.47	0.499238
KAFB-106104/1	4854.961	4854.58	0.380938
KAFB-10611/1	4856.623	4856.67	-0.04744
KAFB-10612/1	4856.501	4856.53	-0.02854

KAFB-10613/1	4855.925	4856.52	-0.59471
KAFB-10614/1	4856.659	4856.78	-0.12082
KAFB-10615/1	4853.751	4854.12	-0.36902
KAFB-10616/1	4857.79	4858.19	-0.40045
KAFB-10617/1	4855.547	4855.4	0.146875
KAFB-10618/1	4855.473	4855.61	-0.13686
KAFB-10619/1	4855.973	4855.58	0.392656
KAFB-1062/1	4856.886	4857.81	-0.92426
KAFB-10620/1	4855.581	4855.65	-0.06943
KAFB-10621/1	4854.986	4855.21	-0.22416
KAFB-10622/1	4854.371	4854.25	0.121094
KAFB-10623/1	4854.976	4854.94	0.035586
KAFB-10624/1	4857.209	4857.13	0.078984
KAFB-10625/1	4853.837	4853.81	0.026914
KAFB-10626/1	4852.388	4852.55	-0.1623
KAFB-10627/1	4858.454	4858.54	-0.0859
KAFB-10628/1	4856.364	4856.3	0.064258
KAFB-1063/1	4856.912	4858.24	-1.32838
KAFB-1064/1	4856.887	4857.29	-0.40279
KAFB-1065/1	4856.369	4856.86	-0.49086
KAFB-1066/1	4856.324	4856.99	-0.66578
KAFB-1067/1	4856.004	4857.17	-1.16561
KAFB-1068/1	4855.999	4856.84	-0.84098
KAFB-1069/1	4856.021	4856.57	-0.54852

EPA United States Environmental Protection Agency

4.2. Goal 1: Mass Transport (MT3DMS)

(Predict the concentrations of EDB that would be expected to reach production wells (i.e., ABCWUA, Kirtland AFB, and VA wells) if nothing was done to mitigate the problem)

Results of the modeling analysis for goal 1 show that EDB is predicted to reach the VA hospital production well, Ridgecrest-5, KAFB-3, and Ridgecrest-3, in this order, assuming there are no hydraulic controls, hydraulic changes, or treatment processes taking place. (These results do not include reactions, decay, or sorption either as explained in the conceptual model.) Less likely impacts are predicted at Ridgecrest 2 and 4 as determined through the sensitivity analysis, although these impacts would require changes in groundwater gradients. Table 9 provides calculated times for EDB to reach production wells at a concentration of 0.05 µg/l, the maximum concentration level (MCL), and also shows the times required for each well to reach its highest concentration of EDB.

Table 9: Predicted EDB Concentrations Reaching Drinking Water Production Wells
(concentrations and times are approximate)

	VA Well	RIDGECREST-5	KAFB-3	RIDGECREST-3
Years to Reach MCL[a] (0.05 µg/l)	2-3	32	41	71
Maximum Concentration	1.09 µg/l	1.69 µg/l	0.17 µg/l	0.52 µg/l
Years to Maximum Concentration	7	64	54	75[b]

a: MCL's are the highest levels of contaminants allowed in drinking water.
b: end of model run

Results show that the MCL for EDB would be detected in the VA hospital production well in approximately 2-3 years, and the highest concentration (1.09 µg/l) would be reached after 7 years. The VA hospital production well may avoid impacts by higher concentrations of EDB because higher concentrations occurring in the central part of the EDB plume move towards the northeast instead of towards of the VA hospital production well. Results also show concentrations in the VA hospital production well

EPA United States Environmental Protection Agency

decreasing from the highest concentration back to the MCL after 24 years. The decrease is caused by simulated diminishing EDB concentrations in the LNAPL source area and bulk plume movement being to the northeast.

Perspectives on EDB plume movement in relation to the VA hospital production well are illustrated by figures 15 and 16. Each figure shows an isosurface where the surface concentration is equal to the MCL. The isosurface in figure 15 represents the current time and shows there is no contact of EDB with the VA hospital production well screen. After 3 years, the isosurface moves to the west and downward to come into contact the upper part of the VA hospital production well screen (fig 16).
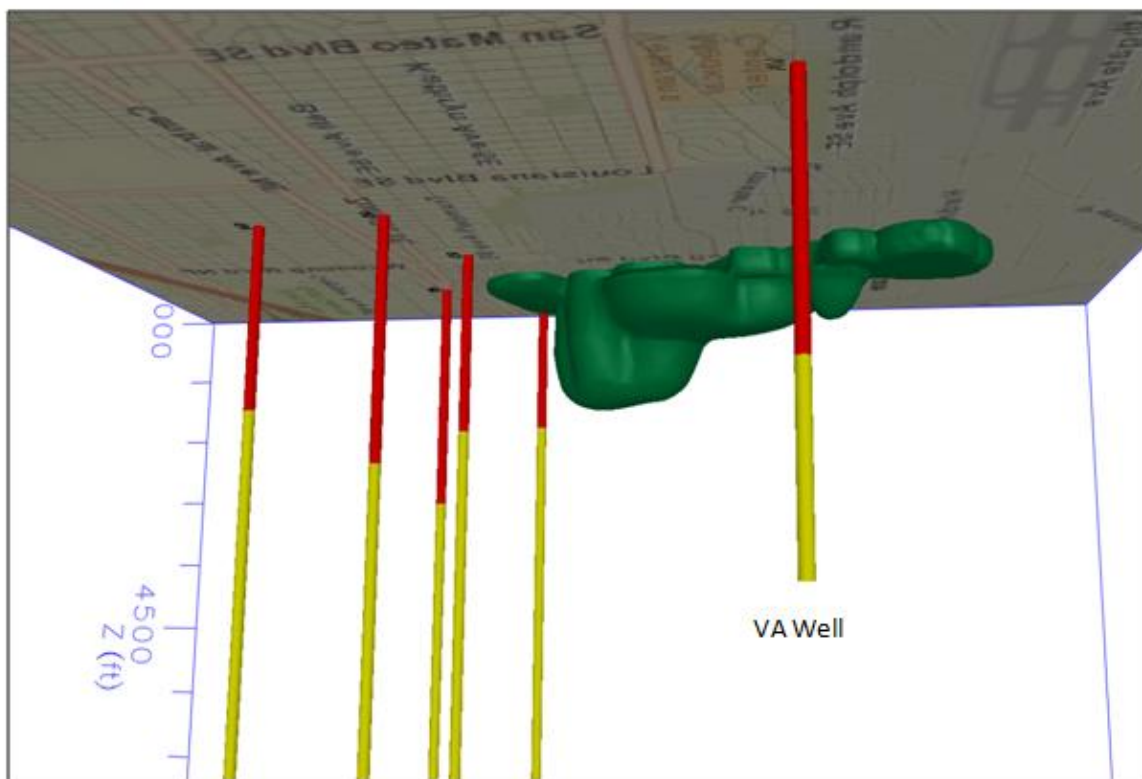

Figure 15: Isosurface position in relation to VA hospital production well.
Subsurface view to the east-northeast. Ridgecrest well field (5-wells) shown on left side of figure. Well screens in yellow.

Well Ridgecrest-5 shows EDB impacts at the MCL occurring in approximately 32 years. The highest concentration of 1.69µg/l is reached at 64 years, and then concentrations decrease to 0.76µg/l at 75 years. KAFB-3 shows the MCL being reached

EPA United States
Environmental Protection
Agency

after 41 years, and the highest concentration (0.17 µg/l) after 54 years. Concentrations in KAFB-3 decrease back to the MCL at 75 years. Ridgecrest-3 shows impacts at the MCL after 71 years. The highest concentration effecting Ridgecrest-3 was not determined because the mass transport model was run to only 75 years. However, at 75 years the concentration is above the MCL at 0.52 µg/l.

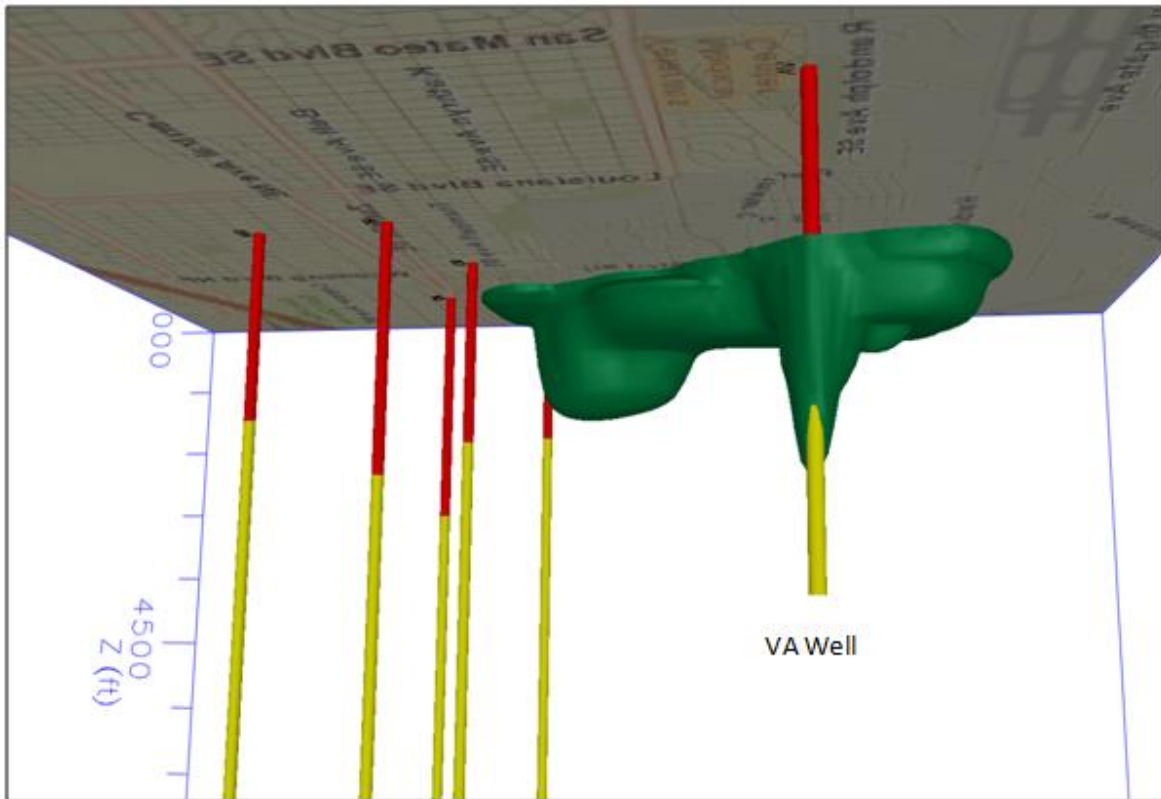**Figure 16: Isosurface after 3 years.**

4.3. Goal 2: Plume Capture (MT3DMS)

(Model a capture zone of two proposed extraction wells associated with an LNAPL containment system)

The purpose of this section is to provide an idea of the types of pumping designs that would be necessary for obtaining hydraulic control of the EDB plume. The recovery well locations, rates, etc. presented here are not the only possibilities, however.   A

greater level of analysis would be necessary before any final designs are determined. No in-situ EDB plume treatment or monitored natural attenuation approaches are included in this capture analysis.

The following capture analysis begins with an evaluation of the capture zone for well KAFB-106157, referred to as the LNAPL recovery/containment well. KAFB-106157 has been installed, but is not currently pumping at the site. As discussed in Section 1.3, because of the governing equations used for contaminant transport modeling, the modeled capture zone for KAFB-106157 is appropriate for dissolved contamination but not LNAPL. In addition, the capture zone evaluation was made using only one recovery well, which is consistent with current site plans.

Next, pumping was evaluated for controlling plume movement towards the VA hospital production well, Ridgecrest wells 5 and 3, and KAFB-3. These pumping designs were determined mainly by trial and error, whereby numerous model runs were conducted while adjusting locations of recovery wells, their pumping rates, and screened intervals until EDB plume movement was controlled. Controlled is used to mean that these production wells were not reached by concentrations of EDB at the MCL or greater. An evaluation of controls for concentrations less than the MCL was not performed, but could be included in supplemental modeling if necessary.

4.3.1. KAFB-106157 (LNAPL Recovery Well)

KAFB-106157 is just north of the LNAPL zone. KAFB-106157 was pumped at 75 gpm based on pumping rate information provided by NMED. This pumping only simulates groundwater flow (not LNAPL capture). The effect of pumping on LNAPL behavior was beyond the scope of modeling capabilities, but should be included as part of a remedial design.

Particle tracking pathlines delineated the capture zone created by KAFB-106157 (fig 17A). The simulated capture zone encompassed less than approximately one-half (42%) of the area along the constant concentration boundary front. The width of the simulated capture zone is approximately 586 ft, while the width of the constant concentration boundary is 1,365 ft. (fig. 17B). To increase capture along the boundary,

one option is to install two additional recovery wells located west of KAFB-106157 (fig 17C). These simulated wells are referred to as "source area 1" and "source area 2" in the model. With the inclusion of these two additional recovery wells, which are each pumping 70 gpm from layer 3 (the EDB shallow zone), capture along the entire boundary was accomplished in the model.

The pumping rate and hydraulic conductivity are both important to the size of the capture zone created by KAFB-106157. For example, if additional aquifer testing determines that hydraulic conductivity is lower than expected, the capture zone will be larger; and if hydraulic conductivity is determined to be higher than expected, the capture zone will be smaller. This assumes the pumping rate is the same in both cases. If the pumping rate changes, then the size of the capture zone would also change. Pumping tests may be necessary near the north end of the LNAPL area to narrow the range of design parameters for developing hydraulic controls.
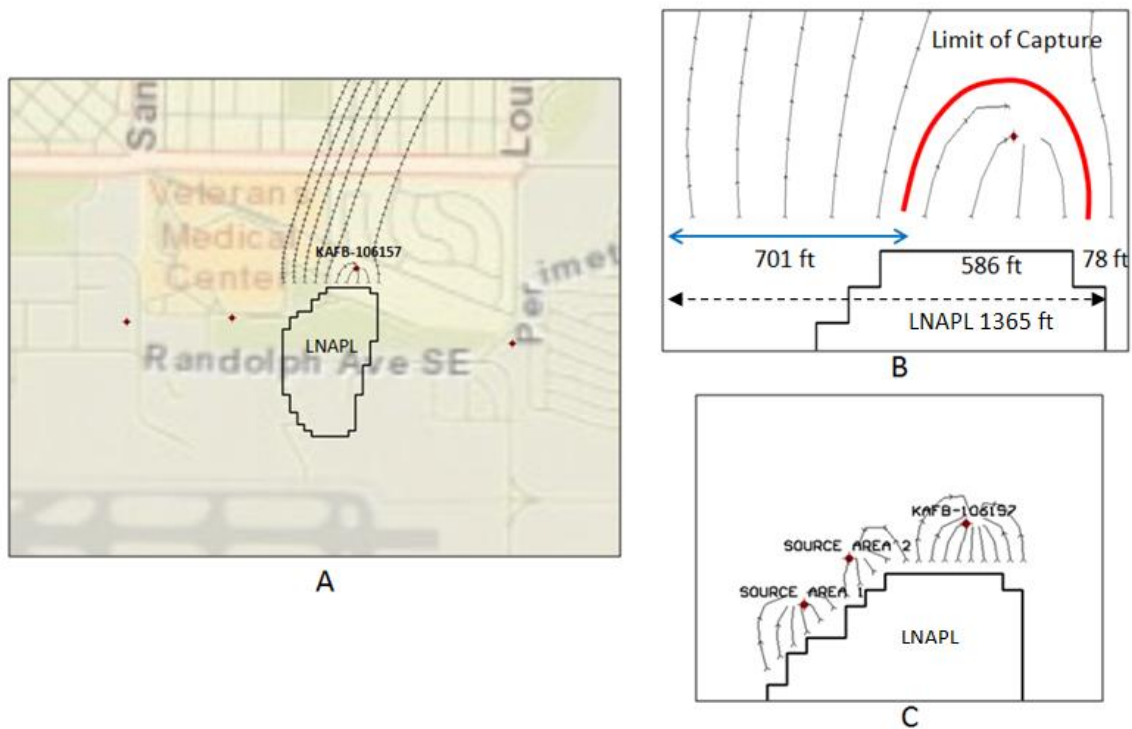

Figure 17: Capture zone for LNAPL/EDB source area.
(A) Particle pathlines shown in relation to LNAPL area; (B) Capture limit of KAFB-106157 zone shown by red curve; and (C) Capture zones created by two additional simulated recovery wells.

4.3.2. Simulated West Recovery Wells

Three simulated recovery wells were placed near the EDB plume's western side for the purpose of examining the potential for establishing hydraulic control of the part of the EDB plume near the VA hospital production well. These wells are shown in figure 18 as west recovery wells 1, 2, and 3, and are each screened in model layers 3-5. Model runs were then performed using pumping rates ranging from 80 to 300 gpm.

Results suggest that difficulties could be encountered in developing hydraulic control sufficient to protect the VA hospital production well. The three recovery wells were not effective at stopping horizontal EDB plume movement within the range of pumping rates tested. Even with pumping rates as high as 300 gpm, the three recovery wells exhibited little effect on horizontal plume movement. Simulated groundwater velocities between the western edge of the plume and the VA hospital production well are relatively high (approximately 0.75 ft/d to just over 1.0 ft/d), in general.
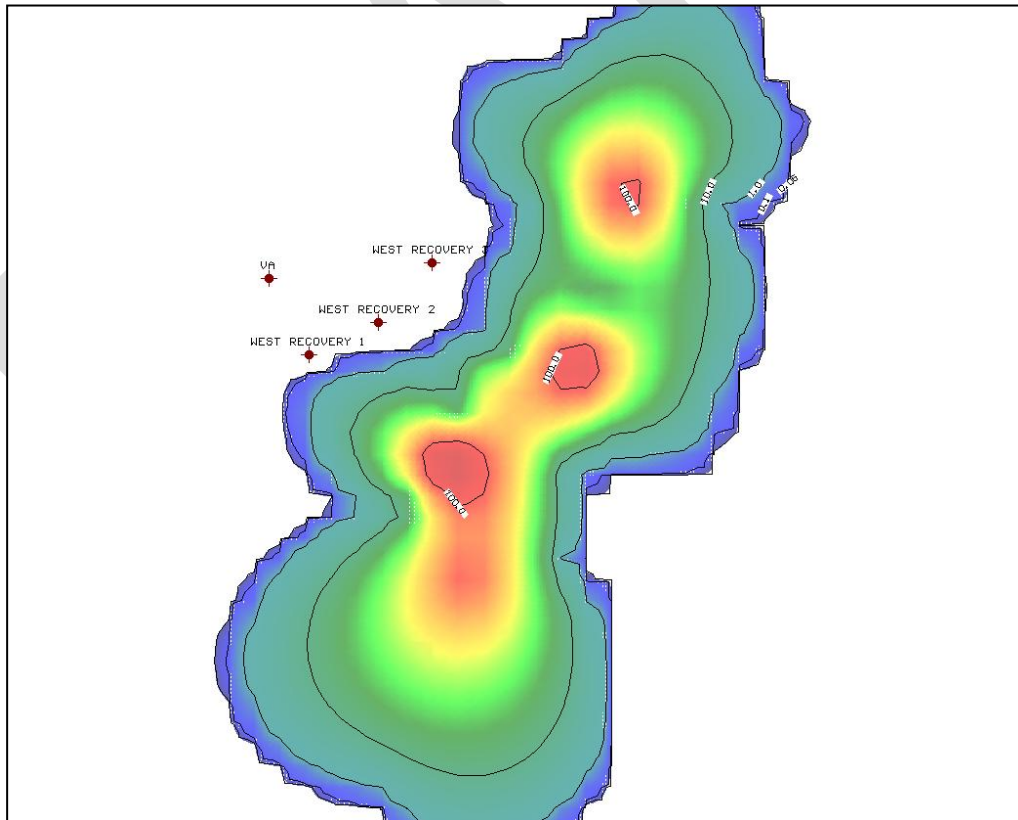

Figure 18: Location of simulated recovery wells for testing west side hydraulic control.

EPA United States Environmental Protection Agency

More promising results were shown for vertical hydraulic control. The three recovery wells obtained marginal vertical hydraulic control with pumping rates as low as 80 gpm. At 80 gpm, the EDB plume still moved horizontally but did not move deeply enough to enter the VA hospital production well screen. The reason is because the recovery wells counteracted the normal vertical gradient caused by the VA hospital production well. Figure 19 illustrates the effects of the three recovery wells pumping at 80 gpm.

There are a number of uncertainties related to model setup that influence EDB transport and capture near the VA hospital production well. These are discussed in Section 5.
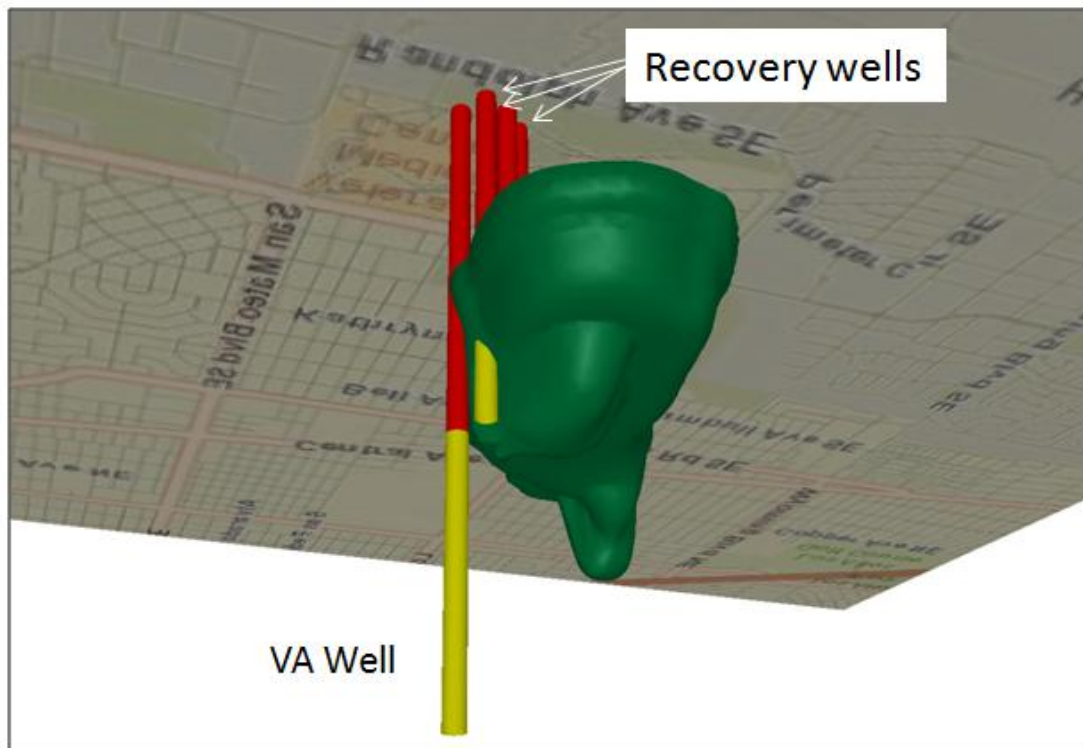

Figure 19: Isosurface (0.05 µg/l) after 5 years; pumping rate 80 gpm.
Subsurface view to the northeast. Well screens in yellow.

4.3.3. Simulated North Recovery Wells

Simulated recovery wells were placed near the plume front to consider basic concepts on the types of pumping designs that would be needed to stop EDB from

moving further towards the Ridgecrest well field. Recovery wells were placed in the model in sets of three, six, and twelve wells, which were then pumped at different rates for each set.

The design using six recovery wells is shown in figure 20. These six wells were placed along the curvature of the plume front similar to a single row of recovery wells. There were assigned pumping rates of 125 gpm each. Using these six recovery wells, results show that no EDB (at the MCL or greater) advanced to Ridgecrest wells 5 and 3 or to any other wells in the Ridgecrest well field, and none advanced to production well KAFB-3 over the 75-year mass transport analysis. Figure 21 shows the beginning position of the EDB plume in relation to these recovery wells, and figure 22 shows the position of the plume after 25 years.
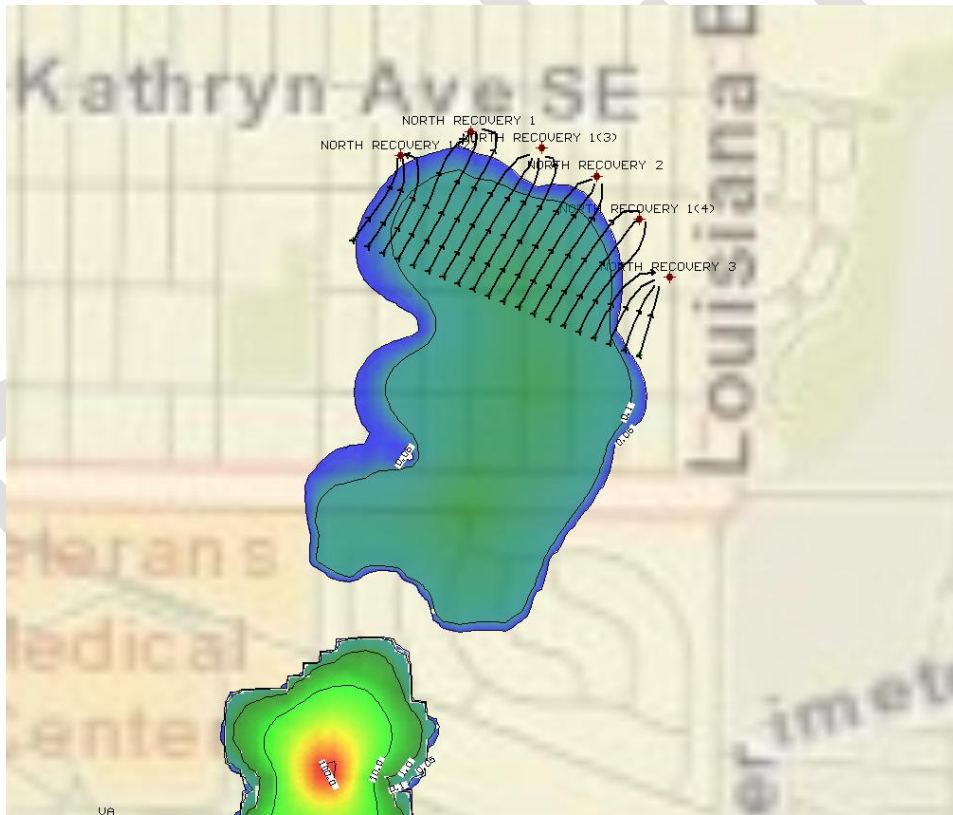
Figure 20: Simulated recovery wells and capture zones near the Ridgecrest well field.
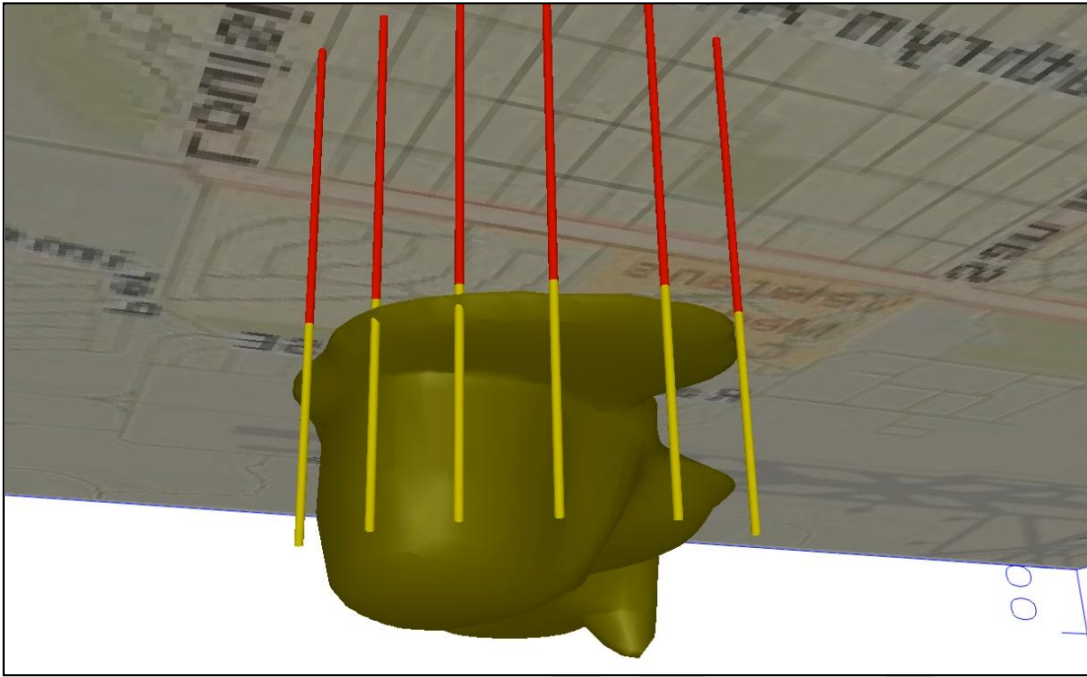
United States
Environmental Protection
Agency

Figure 21: Recovery wells and EDB plume at start of model run.
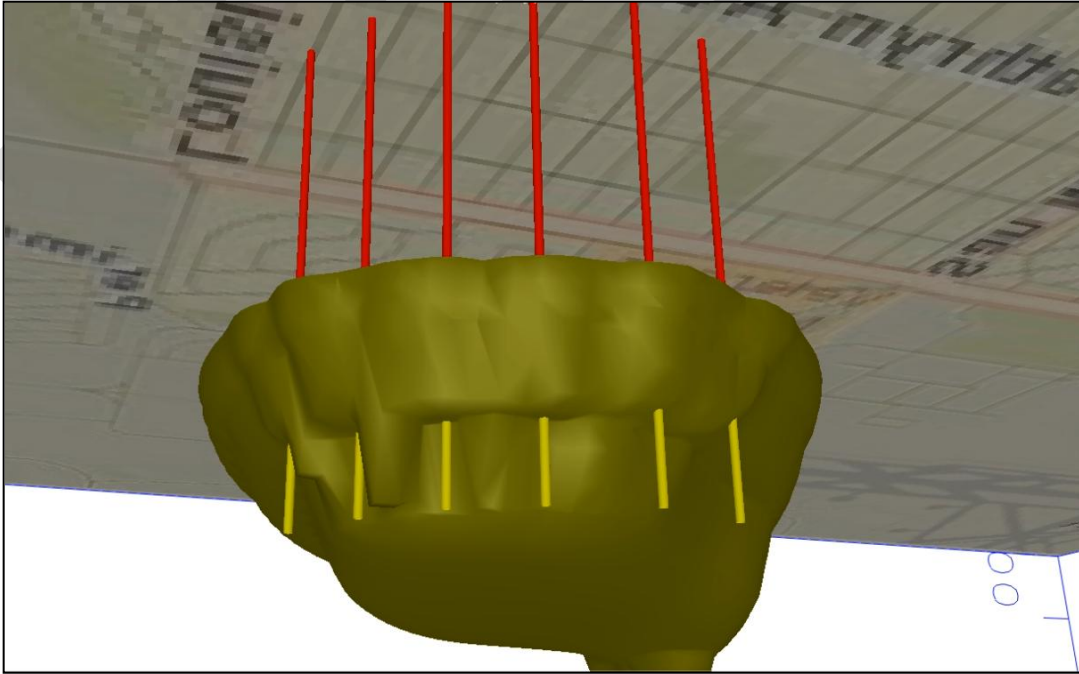View to the southeast.

Figure 22: Plume at approximately 25 years.
View to the southeast

Next, twelve recovery wells were placed into the model in locations following the curve of the plume front similar to the six recovery wells used previously (fig. 23). This design essentially formed two rows of six recovery wells per row. These twelve recovery wells were pumped in two different ways: (i) by using higher pumping rates on the east side than on the west side (125 gpm on the east, and 60 gpm on the west), and (ii) by using the same pumping rates in all twelve wells (100 gpm). The reason for testing higher pumping rates on the east is because earlier model runs indicated that bulk plume movement seemed to be greater on the east side than on the west, suggesting that higher pumping rates would be needed on the east but reduced rates would be more efficient on the west.

Of the two pumping scenarios described above (i and ii), using 100 gpm for all twelve recovery wells was successful in stopping plume advancement. The test using the 125-60 gpm rates stopped most of the plume, but some EDB moved east around the recovery wells and further towards the Ridgecrest well field.
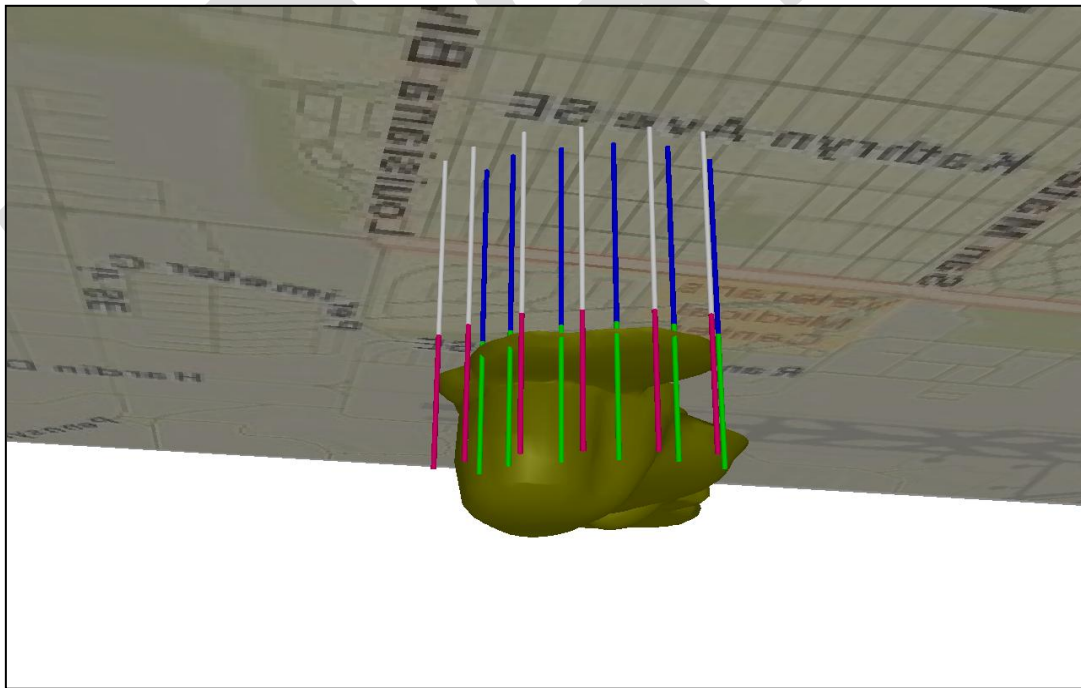

Figure 23: Recovery wells placed in two rows of six.

United States
Environmental Protection
Agency

Recovery wells for the three-well test are shown in figure 24. These three wells are labeled as north recovery 1, north recovery 2, and north recovery 3. Pumping rates for north recovery wells 1 and 3 were 125 gpm, and the pumping rate for well north recovery 2 was175 gpm. The rates for north recovery wells 1 and 3 were less than north recovery well 2 to try and increase efficiency (by pumping less uncontaminated water) on the edges of the plume. However, results show that the plume was not contained by these three wells and that EDB moved past recovery wells towards the Ridgecrest well field.
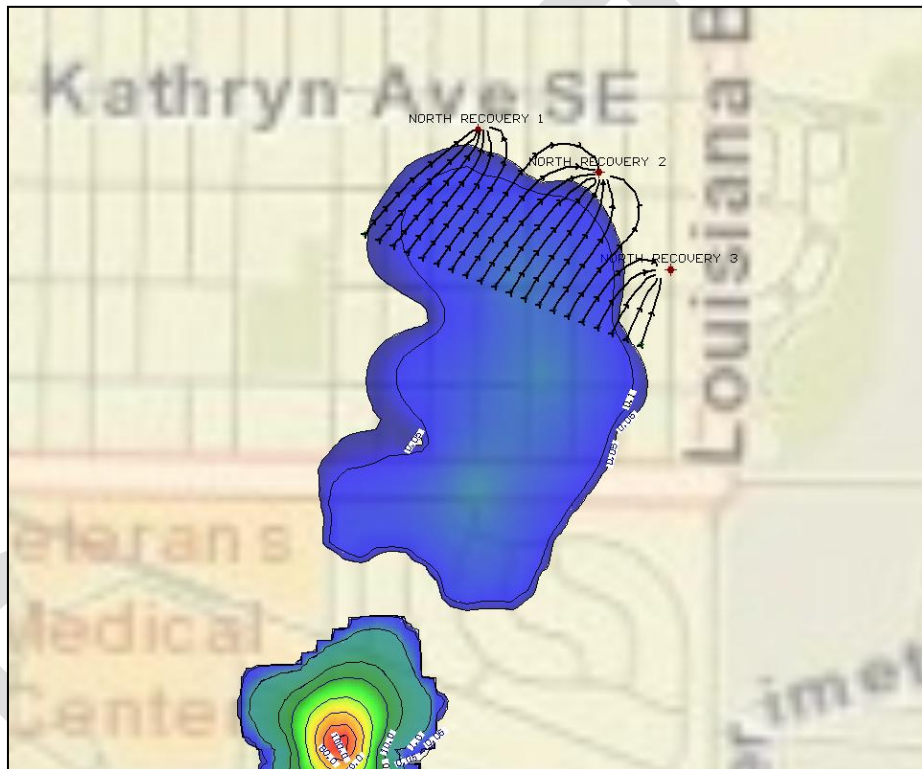

Figure 24: Test for plume recovery using three simulated recovery wells.

The above tests suggest a collective pumping rate between approximately 750 gpm to 1,200 gpm, distributed generally even between recovery wells, appears to provide sufficient hydraulic control of the plume front.

5.   MODEL UNCERTAINTIES AND SENSITIVITIES

5.1.   Uncertainties

The discussion of modeling uncertainties is included to describe the main uncertainties that were encountered and how they were addressed. Uncertainties were caused by data gaps which required making assumptions during model construction and the setup of individual model runs. Uncertainties were addressed by considering all available site-specific and/or regional data, as appropriate, and by using such information with professional judgment and reviews to bridge data gaps and produce reasonable model output. The main uncertainties involve groundwater monitoring coverage, values for specified head boundaries, future groundwater pumping rates and well locations, potential installation of recovery wells, and data for model validation.

5.1.1.   Groundwater Monitoring Coverage

Like many groundwater models, this model uses monitoring wells clustered in the area of concern. Clustered data points in modeling are common because field investigations are not typically designed at the outset to support modeling efforts. Ideally, groundwater monitoring wells should be distributed throughout a model domain. Although the flow model achieved acceptable matching between calculated and observed heads, there are areas of the model domain where no monitoring wells exist so it was not possible to calibrate heads in those areas. The significance is that simulated flow directions are potentially less reliable at distances away from existing groundwater monitoring wells.

A related reason for having monitoring well data gaps is that the scale of the model had to encompass an area larger than the EDB plume. The larger area was necessary to include the Ridgecrest well field and other pumping wells in southeast Albuquerque. These pumping wells had to be included to create the appropriate flow field and to assess the movement of the EDB plume towards pumping wells. Additional groundwater monitoring wells or piezometers placed north and northeast of the Ridgecrest well field would improve flow model accuracy.

There are several factors that helped offset uncertainties caused by the lack of monitoring well coverage. First, there is good calibration where monitoring wells exist, and thus there is a high-level of confidence in groundwater flow directions in the central part of the model domain. Second, flow directions from the larger/preliminary model domain used early in the project, and flow directions in the final smaller model domain, are generally consistent. Head calibration in the larger early model included head data from USGS wells more widely distributed over southeast Albuquerque, and resulted in a normalized RMS of around 15%. Finally, the overall groundwater gradients produced by the model are similar to flow gradients noted on maps in previously published groundwater studies.

5.1.2. Specified Head Boundaries

Hydraulic head and linear gradients assigned to specified head boundaries are not calibrated to actual measurements because monitoring wells do not exist where specified head boundaries are located. If actual head values at the boundaries were known, simulated flow directions would have been more accurate. Boundary head on the north and east sides of the model are especially important to determining the timing of when the EDB plume will reach Ridgecrest-5 and Ridgecrest-3. There are only several groundwater monitoring wells around the edges of the model domain that could be used to provide head data for boundary conditions.

The final conditions of specified head boundaries were based on achieving successful head calibration. Boundary values were adjusted until matching of calculated and observed hydraulic head measurements resulted in a normalized RMS of 10% or less. Since there were few actual measurements near specified head boundaries, boundary values were initially estimated by using data from published groundwater maps, and by using head output derived from the earlier larger model domain.

5.1.3. Future Groundwater Pumping

Since the mass transport model involves long-term predictions about contaminant transport and concentrations, it is important to keep in perspective that future changes in

local and regional groundwater gradients caused by changes in pumping, new wells or well replacement, or other related reasons would probably decrease the relevancy of current model results. If changes are planned in advance and the locations and pumping rates of future production wells are known, the model can be revised to include those planned changes to provide updated model predictions. A transient model of EDB plume movement could also be developed to evaluate EDB plume movement under variable hydraulic conditions related to changes in regional groundwater levels, and possible alternative pumping scenarios, assuming necessary model data are available.

5.1.4. Potential Installation of Recovery Wells

While the model demonstrated that hydraulic control is obtainable through the use of recovery wells, it is beyond the scope of this project to address many real-world considerations necessary for installing new wells. The EDB plume capture component of this model is simply a means to evaluate the effects of simulated recovery wells with regard to achieving hydraulic control.

The model could not address any engineering, financial, logistical, or other related factors involved with the installation, development, operation, and maintenance of recovery wells. It is also unclear whether feasible options exist for treating and handling potentially large volumes of groundwater produced by any newly installed recovery wells. However, without the installation of recovery wells, hydraulic control will not be obtained and the likelihood of EDB reaching drinking water production wells remains high.

5.1.5. Reduction in EDB Concentration at LNAPL Area

The LNAPL area was treated as an EDB concentration boundary where the concentration decreases at a rate of 10% per year. While it is not certain that this rate can be achieved, it would also be uncertain, for example, to use a boundary condition that remains unchanged for the 75 year model time (i.e., providing a constant concentration of EDB for 75 years). However, running the model using a boundary that provides a constant concentration of EDB, or other variations in concentration boundary changes,

are still options, if those modeling goals are determined. Future sampling data should provide better indications of changes in EDB concentrations at the LNAPL area.

5.1.6. EDB Plume Movement/Capture Near the VA Hospital Production Well

Results related to the VA hospital production well should be carefully interpreted. This is because the ratio of horizontal to vertical hydraulic conductivity, the ratio of horizontal to vertical dispersion, grid cell size, and the distance between the EDB plume are all modeling factors that influence the rate of EDB movement and capture near the VA hospital production well. A more extensive analysis of these factors is needed to improve the confidence of model predictions in this area.

5.1.7. Data for Model Validation

Model validation compares model predictions to actual measurements outside the data sets used for model calibration. At this time, no data sets exist for model validation and model validation has not been performed. It is not uncommon for models to not undergo validation. Collecting data for validation usually requires additional time and resources that are sometimes not available. When collecting additional data is not possible, alternative approaches to validation can sometimes be developed including the use of historical data. Alternatives to customary model validation can be discussed with NMED if necessary.

5.2. Sensitivities

The emphasis of the sensitivity analysis was on evaluating how sensitive groundwater flow and plume movement is to changes in model inputs for boundary heads and pumping rates. Sensitivities were examined by systematically modifying boundary heads and pumping rates. Model sensitivities were evaluated first by determining whether flow sensitivities are significant according to ASTM Standard Guide D5611-94 (ASTM, 2008b). If groundwater flow sensitivities were found to potentially invalidate flow model results, a sensitivity analysis was then performed for plume movement. Sensitivity to hydraulic conductivity was not evaluated because the field of hydraulic

conductivity in the model was determined during planning discussions with NMED. However, sensitivity to hydraulic conductivity can still be conducted later, if necessary.

ASTM recommends classifying groundwater flow sensitivities as a Type I, II, III, or IV sensitivity, depending on whether the changes to the calibration residuals and modeling conclusions are significant or insignificant when inputs are changed. The ASTM classifications are summarized below:

Type I: Occurs when variation of an input causes insignificant change in calibration as well as the model's conclusions. *Type I is of no concern because regardless of the value of the input, the conclusions are the same.*

Type II: Occurs when variation of an input causes significant changes in the calibration but insignificant changes in the model's conclusions. *Type II is of no concern because regardless of the input the conclusions remain the same.*

Type III: Occurs when variation of an input causes significant changes to both calibration and the model's conclusions. *Type III is of no concern because, even though the model's conclusions change as a result of variation, the parameters cause the model to become uncalibrated and eliminates those values from being considered as realistic.*

Type IV: Occurs when a variation causes changes in model conclusions but the change in calibration is insignificant. *Type IV can invalidate model results because over the range of that parameter in which the model can be considered calibrated, the conclusions of the model change.*

5.2.1. Sensitivity Test Methodology

Groundwater flow sensitivities were evaluated according to the following procedure. During the procedure if a type IV sensitivity was identified, additional evaluations were then performed on plume movement for the related flow scenario. The additional analyses involved performing mass transport model runs to examine

differences in travel times and concentrations of EDB. Particle travel times were used to screen for possible changes in EDB transport mass transport sensitivities were evaluated. **Discussions below for mass transport are in bold.**

Procedure

- **Step 1**: A uniform change was applied to all boundary heads by increasing and decreasing all heads by 5, 10, and 15 feet. Model run iterations were then performed to obtain the normalized RMS and correlation coefficient. Flow directions and particle travel times to selected production wells were examined. The selected wells were Ridgecrest 3 and 5.

- **Step 2**: Changes in heads were applied to north and east boundaries by alternating increases and decreases by 10 feet for each boundary. Changes to the north and east boundaries were examined specifically because those boundaries are closest to the Ridgecrest well field and have greater influences over groundwater flow in the immediate area.   Calibration statistics, flow directions, and particle travel times were noted.

- **Step 3**: The pumping rates for wells Ridgecrest 3 and 5 were increased and decreased by 25% while leaving boundary heads in their original condition. Pumping changes were alternated between the two wells. Calibration statistics, flow directions, and particle travel times were noted.

5.2.2. Sensitivity Test Results

Step 1

The uniform changes applied to boundary heads in step 1 resulted in corresponding significant changes to the normalized RMS, but the correlation coefficients, particle travel times, and flow directions were mainly unchanged (table 10). Because there are significant changes to model calibration but the groundwater flow regime overall remained the same, this was rated as a type II sensitivity. No further analyses were performed for step 1.

Table 10: Step 1 Sensitivity Test Results
Uniform Changes to Boundary Head

Sensitivity Test	Boundary Head Change (ft)	Normalized RMS	Correlation Coefficient	Earliest Particle Arrival at Ridgecrest-5[a] (~yr)	Earliest Particle Arrival at Ridgecrest-3[b] (~yr)	Observed Changes to Flow Directions
1a	+5	70.48	0.95	21	70	minor
1b	+10	137.08	0.96	20.8	70	minor
1c	+15	203.49	0.96	21.1	68.5	minor
1d	-5	63.5	0.96	20.6	70	minor
1e	-10	130.17	0.96	21	71.2	minor
1f	-15	217.41	0.95	20.5	*	minor

a: Particle travel in layer 8.
b: Particle travel in layer 3
* Heads below layer bottom; particle tracking not calculated.

Step 2

Changes to the north and east boundaries caused changes to groundwater flow conclusions for two of the four sensitivity tests performed in step 2 (table 11). When head was increased on the eastern boundary (test 2b), all particles arrived at Ridgecrest-5 including particles in layer 3. When head at the north boundary was decreased (test 2c), a steeper northerly groundwater gradient was created as well as a smaller capture zone for Ridgecrest-5. Because of the smaller capture zone, some particles previously captured by Ridgecrest-5 were able to move further northward and arrive at Ridgecrest-4. Because the normalized RMS remained relatively low even with these changes to conclusions, these sensitivities were rated as type IV. Additional analysis of plume movement for tests 2b and 2c were thus performed using the mass transport model.

For test 2b, mass transport indicates that Ridgecrest-5 would be impacted by EDB in ~30 years. However, at ~30 years, EDB is not completely captured by Ridgecrest-5 and it moves further north and east into the area central to Ridgecrest

wells 3, 4, and 5. By activating the six simulated recovery wells, hydraulic control was maintained and there were no impacts to any of the Ridgecrest wells for test 2b.

Table 11: Step 2 Sensitivity Test Results
Changes to North and East Boundary Head

Sensitivity Test	Boundary Head Change (ft)		Normalized RMS	Correlation Coefficient	Earliest Particle Arrival at Ridgecrest-5[a] (~yr)	Earliest Particle Arrival at Ridgecrest-3[b] (~yr)	Observed Changes to Flow Directions
2a	North	+10	28.70	0.95	30	49.3	minor
	East	+ 0					
2b	North	+ 0	16.53	0.95	22.5	No arrival; all particles arrived at Ridgecrest-5	more westerly
	East	+ 10					
2c	North	- 10	21.85	0.96	17.53	no arrival at Ridgecrest-3; arrival at Ridgecrest-4 at 60 yrs	Steeper gradient causes some particles to move past Ridgecrest-5
	East	- 0					
2d	North	- 0	10.23	0.96	20	46.58	minor
	East	- 10					

a: Particle travel in layer 8
b: Particle travel in layer 3

The mass transport model for sensitivity test 2c shows that a decrease in head at the north boundary will cause the EDB plume move past Ridgecrest-5. Upon activation of the six recovery wells, the combined effect of the lower head boundary and activated recovery wells caused heads in layer 3 to fall below the bottom of grid cells, producing "dry cells" and thus unclear results for contaminant transport in the shallow zone.

Step 3

The model showed little sensitivity to increasing and decreasing pumping rates in Ridgecrest-5 (tests 3a and 3b), as indicated by relatively consistent values for the normalized RMS, particle arrival times, and only minor changes in flow directions (table 12). Tests 3a and 3b were rated as type I sensitivities and no further analyses were

EPA United States Environmental Protection Agency

performed. Similarly, an increased pumping rate in Ridgecrest-3 also resulted in a type I sensitivity (test 3c).

A decreased pumping rate in Ridgecrest-3 showed more significant changes (test 3d). Although the normalized RMS was consistent with other tests, the flow direction was more westerly. This was rated as a type IV sensitivity thus warranting an analysis of mass transport.

Mass transport results for test 3d show EDB in close proximity, but not reaching, Ridgecrest-3 at ~75 years. If the model run time were slightly longer, EDB would most likely have reached Ridgecrest-3. Results also show the plume spreading between Ridgecrest-3 and Ridgecrest-2.

Table 12: Step 3 Sensitivity Test Results
Changes to Pumping Rates

Sensitivity Test	% Change in Pumping Rate	Normalized RMS	Correlation Coefficient	Earliest Particle Arrival at Ridgecrest-5[a] (~yr)	Earliest Particle Arrival at Ridgecrest-3[b] (~yr)	Observed Changes to Flow Directions
Ridgecrest-5						
3a	+25	6.07	0.96	18.9	76.7	minor
3b	-25	9.09	0.96	23.3	63.0	minor
Ridgecrest-3						
3c	+25	6.12	0.96	20	52.5	minor
3d	-25	8.56	0.96	21.6	no arrival at Ridgecrest-3; movement towards Ridgecrest-5	more westerly

a: Particle travel in layer 8
b: Particle travel in layer 3

6. RECOMMENDATIONS FOR ADDITIONAL MODELING

There are a number of modeling scenarios that would provide useful information about EDB movement and control, but are beyond the scope of current modeling goals. These include simulating the effects of combinations of recovery and injection wells, deactivating certain production wells (Ridgecrest wells or others), delineating vertical intervals of the aquifer that contribute both more and less groundwater to production wells, and exploring options for transient modeling.

Given that plume control would require pumping (extracting), treating, and presumably injecting large quantities of treated groundwater, injecting treated water would be important to local hydrology and plume movement depending on injection well location(s) and injection rates. Injection and pumping wells could be used in a number of schemes, such as described in pump and treat design guidelines by Cohen and others (1997). Pumping and injection systems should be simulated before installation to help understand potential effects on EDB plume movement.

In the event EDB is detected in production wells, turning off affected wells may be considered. In order to assist with contingency planning, additional model runs could be performed to see how the plume reacts to deactivating production wells, and whether that would put any other production wells at greater risk of becoming contaminated.

Hydrogeologic studies of the Albuquerque area have shown that some intervals of the Santa Fe Group aquifer system are more transmissive of groundwater than others. Although not enough of this type of hydrogeologic information was identified for use in the current model, it could be included in the future if available. The model could be refined by modifying layer properties, or including additional layers, to represent strata contributing the most water to production wells.

Finally, transient modeling may be possible (i.e., where model boundaries, pumping, and other conditions change over time), but model setup would require accurate projections for groundwater conditions in the future. Transient models have advantages in that more realistic boundary conditions can be included, but they are more complex to arrange and will not necessarily decrease any modeling uncertainties.

&EPA United States
Environmental Protection
Agency

7. CONCLUSIONS

Modeling results showed that without any hydraulic or other controls in place, simulated EDB concentrations at the MCL (0.05 µg/l) reached drinking water production wells in the Ridgecrest well field in approximately 30 years (for Ridgecrest-5), and in approximately 70 years (for Ridgecrest-3). Similarly, results show well KAFB-3 being reached in approximately 40 years, and the VA hospital production well being impacted in only 2-3 years. Predicted impacts to the VA hospital production well are less certain than for other production wells because of factors related to model setup (possibly numerical dispersion). Lateral expansion of the EDB plume to the east and west resulted in EDB reaching KAFB-3 and the VA hospital production well, although bulk plume movement is towards the Ridgecrest well field. Concentrations of EDB reaching simulated drinking water production wells were relatively low and remained under 2.0 µg/l.

Impacts to drinking water production wells were avoided by using simulated recovery wells. Sets of simulated recovery wells placed at the north end of the EDB plume, with wells pumping between 100 and 125 gpm each, were effective at protecting the Ridgecrest well field under most groundwater flow scenarios tested. Protection of the VA hospital production well was only marginally successful, but vertical control was obtained using recovery well pumping rates of 80 gpm. Simulated recovery wells placed just north of the LNAPL area and pumping 70 gpm each, coupled with simulated decay of EDB concentrations in LNAPL, were effective at cutting off the EDB plume from its source.

How the groundwater system at large is managed in the future will influence the effectiveness of any hydraulic controls. If it is determined that hydraulic controls will be implemented as part of a remediation system, it is recommended that a controls be developed as part of a groundwater management plan to monitor for changes in local and regional groundwater gradients.

8. REFERENCES

ABCWUA, 2011 Water Quality Report.

Allen and others, 1998, Core drilling provides information about Santa Fe Group aquifer system beneath Albuquerque's west mesa, New Mexico Geology, February, 1998.

Anderson M.P., and Woessner, W.M., 1992, Applied Groundwater Modeling; Simulation of Flow and Advective Transport: Academic Press, Inc.

Aronson, D., and Howard, P.H., 2008, The environmental behavior of ethylene dibromide and 1,2-dichloroethane in surface water, soil, and groundwater, API publication 4774.

ASTM D 5609-94, Reapproved 2008a, Standard Guide for Defining Boundary Conditions in Ground-Water Flow Modeling.

ASTM D 5611-94, Reapproved 2008b, Standard Guide for Conducting a Sensitivity Analysis for a Groundwater Flow Application.

Balleau Groundwater, Inc., 2002, Model of a perched zone of saturation at Sandia National Laboratories, New Mexico.

Bexfield, L.M., Lindberg, W.E., and Anderholm, S.K., 1999, Summary of water-quality data for City of Albuquerque drinking-water supply wells 1988-97: U.S. Geological Survey Open File Report 99-195.

Bexfield, L.M., and Anderholm, S.K., 2000, Predevelopment water-level map of the Santa Fe Group aquifer system in the middle Rio Grande basin between Cochiti Lake and San Acacia, New Mexico, U.S. Geological Survey Water-Resources Investigations Report 00-4249.

Bexfield, L.M., and McAda, D.P., 2003, Simulated effects of ground-water management scenarios on the Santa Fe group aquifer system, middle Rio Grande basin, New Mexico, 2001-40.

Bexfield, L.M., and Anderholm, S.K., 2002, Spatial patterns and temporal variability in water quality from City of Albuquerque drinking-water supply wells and piezometer nests, with implications for the ground-water flow system: U.S. Geological Survey Water Resources Investigations Report 01-4244.

Bexfield, L.M., Jurgens, B.C., Crilley, D.M., and Christenson, S.C., 2011, Hydrogeology, water chemistry, and transport processes in the zone of contribution of a public-supply well in Albuquerque, New Mexico, 2007-9, U.S. Geological Survey Scientific Investigations Report 2011-5182.

Bjorklund, L.J. and Maxwell, B.W., 1961, Availability of ground water in the Albuquerque area, Bernalillo and Sandoval Counties, New Mexico: New Mexico State Engineer, Technical Report 21.

Centers for Disease Control and Prevention, 2007, NIOSH pocket guide to chemical hazards; publication No. 2005-149.

Chevron, 2003, Material Safety Data Sheet, Aviation Gasoline.

Cohen, R.M., Mercer, J.W., Greenwald, R.M., and Beljin, M.S., 1997, Design guidelines for conventional pump-and-treat systems; U.S. EPA, EPA/540/S-97/504, Office of Research and Development.

Connell, S.D., Allen, B.D., and Hawley, J.W., 1998, Subsurface stratigraphy of the Santa Fe group from borehole geophysical logs, Albuquerque area, New Mexico: New Mexico Geology, Vol 20, No. 1.

Doriski, T.P., Hussain, S., Davis, S.O., and Tsang-Rakovan, M., Conference on geology of Long Island and metropolitan New York, Stony Brook University; April 23, 1009.

Fetter, C.W., 2001, Applied Hydrogeology, 4th ed: Prentice Hall.

Fetter, C.W., 2008, Contaminant Hydrogeology, 2nd ed: Waveland Press, Inc.

Franke, O.L., Reilly, T.E., and Bennett, G.D., 1987, Definition of boundary and initial conditions in the analysis of saturated ground-water flow systems—An introduction; Techniques of water-resources investigations of the United States Geological Survey, Ch B5, Book 3, Applications of Hydraulics.

Falta, R.W., 2004, The potential for ground water contamination by the gasoline lead scavengers ethylene dibromide and 1,2-dichloroethane: Ground Water Monitoring and Remediation 24 no. 3, p 76-87.

Falk, S.E., Bexfield, L.M., and Anderholm, S.K., 2011, Estimated 2008 groundwater potentiometric surface and predevelopment to 2008 water-level change in the Santa Fe Group aquifer system in the Albuquerque area, central New Mexico, prepared in cooperation with the Albuquerque Bernalillo County Water Utility Authority; Scientific Investigations Map 3161.

Gelhar, L.W., Welty, C., and Rehfeldt, K.R., 1992, A critical review of data on field-scale dispersion in aquifers; Water Resources Research, v. 28, p. 1955-1974.

Groundwater Management Inc. (1988), Pumping test data analysis, Ridgecrest well field, City of Albuquerque, N.M.; prepared for Black and Veatch.

Harbaugh, A.W., 1990, A computer program for calculating subregional water budgets using results from the U.S. Geological Survey modular three-dimensional ground-water flow model: U.S. Geological Survey Open-File Report 90-392, 46 p.

Harbaugh, A.W., Banta, E.R., Hill, M.C., and McDonald, M.G., 2000, MODFLOW-2000, the U.S. Geological Survey modular ground-water model -- User guide to modularization concepts and the Ground-Water Flow Process: U.S. Geological Survey Open-File Report 00-92, 121 p.

Hawley, J.W. and Haase, C.S. (compilers), 1992, Hydrogeologic framework of the northern Albuquerque basin: New Mexico Bureau of Mines and Mineral Resources, Open-File Report 387.

Henderson, J.L., Falta, R.W., and Freedman, D.L., 2009, Simulation of the effect of remediation on EDB and 1,2-DCA plumes at sites contaminated by leaded gasoline: Journal of Contaminant Hydrology, 108, pages 29-45.

Kirtland AFB Stage 2 Abatement Plan, 2009, Extraction Well KAFB-ST105-EX01, Aquifer Test Report.

Kirtland AFB site investigation, Quarterly Pre-Remedy Monitoring & Site Investigation Report for July–September 2011; December 2011.

Kirtland AFB site investigation, Quarterly Pre-Remedy Monitoring & Site Investigation Report for July–September 2012; December 2012.

Kirtland AFB site investigation, Quarterly Pre-Remedy Monitoring & Site Investigation Report for October-December 2012; March 2013.

Katz, B.G., 1993, Biogeochemical and hydrological processes controlling the transport and fate of 1,2-dibromoethane (EDB) in soil and ground water, central Florida: U.S. Geological Survey Water Supply Paper 2402.

Kelley, V.C., Woodward, L.A., Kudo, A.M., and Callender, J.F., 1976, Guidebook to Albuquerque basin of the Rio Grande rift, New Mexico: New Mexico Bureau of Mines and Mineral Resources.

Kelley, V.C., 1977, Geology of Albuquerque Basin, New Mexico, New Mexico Bureau of Mines and Mineral Resources, Memoir 33.

Kelley, V.C., 1982, Albuquerque, its mountains, valley, water, and volcanoes: New Mexico Bureau of Mines and Mineral Resources.

Kelly, T.E., 1982, History of water use in the greater Albuquerque area: New Mexico Geological Society Guidebook, 33rd Field Conference, Albuquerque Country II.

Kernodle, J.M., 1998, Simulation of ground-water flow in the Albuquerque Basin, central New Mexico, 1901-95, with projections to 2020: U.S. Geological Survey Open-File Report 96-209.

Kernodle, J.M., McAda, D.P., and Thorn, C.R., 1995, Simulation of groundwater flow in the Albuquerque basin, central New Mexico, 1901-1994, with projections to 2020; U.S. Geological Survey Water Resources Investigations Report 94-4251.

McAda, D.P., and Barroll, P., 2002, Simulation of ground-water flow in the middle Rio Grande basin between Cochiti and San Acacia, New Mexico: U.S. Geological Survey Water-Resources Investigations Report 02-4200.

McKeever, R., Sheppard, D., Nusslein, K., Kyung-Hwa, B., Khalil, R., Ergas, S.J., Forbes, R., Hilyard, M., Park, C., 2012, Biodegredation of ethylene dibromide (1,2-dibromoethane [EDB]) in microcosms simulating in situ and biostimulated conditions: Journal of Hazardous Materials, 209-210, pages 92-98.

National Institutes of Health, 2011, 1,2-Dibromoethane, Report on carcinogens, 12th ed.; National Toxicology Program, Department of Health and Human Services.

Pollock, D.W., 1994, User's guide for MODPATH/MODPATH-PLOT, Version 3: A particle tracking post-processing package for MODFLOW, the U.S. Geological Survey finite-difference ground-water flow model: U.S. Geological Survey Open-File Report 94-464.

Schlumberger Water Services Inc., 2012, Visual Modflow Users Manual.

Source Water Assessment Albuquerque Water Supply System Public Water System No. 107-01, New Mexico Environment Department Drinking Water Bureau March 2002.

Shaw Environmental and Infrastructure, Inc., 2011, Quarterly report 04, bulk fuels facility, Kirtland Air Force Base, New Mexico.

Shaw Environmental and Infrastructure, Inc., 2012, Quarterly report 04, bulk fuels facility, Kirtland Air Force Base, New Mexico.

Spidle, D., Weaver, J., Exum, L., Colon, D., and Burton, S., 2007, Environmental impacts from lead scavengers in avgas and gasoline, U.S. EPA 19th Annual National Tanks Conference and Expo, San Antonio, Tx, March 5-7, 2007.

Thorn, C.R., McAda, D.P., and Kernodle, J.M., 1993, Geohydrologic framework and hydrologic conditions in the Albuquerque Basin, Central New Mexico: U.S. Geological Survey Water Resources Investigations Report 93-4149.

Thorn, C.R., 2000, Results of well-bore flow logging for six water-production wells completed in the Santa Fe Group aquifer system, Albuquerque, New Mexico, 1996-98; U.S. Geological Survey Water-Resources Investigations Report 00-4157.

Thorn, C.R., 2001, Analytical results of a long-term aquifer test conducted near the Rio Grande, Albuquerque, New Mexico; U.S. Geological Survey Water-Resources Investigations Report 00-4291.

USGS National Water Information System, 2012; http://waterdata.usgs.gov/nwis.

U.S. EPA, 2002, Guidance for quality assurance project plans for modeling, QA/G-5M, EPA/240/R-02/007, Office of Environmental Information.

Van Hart, D., 2003, Geologic investigation, an update of subsurface geology on Kirtland Air Force Base, New Mexico; prepared by Sandia National Laboratories, SAND 2003-1869.

Wilson, J.T., Banks, K., Earle, R.C., He, Y., Kuder, T., and Adair, C., 2008, Natural attenuation of the lead scavengers 1,2-Dibromoethane (EDB) and 1,2-dichloroethane (1,2-DCA) at motor fuel release sites and implications for risk management: U.S. EPA, 600/R-08/107.

Woodward, L.A., 1982, Tectonic framework of Albuquerque country: New Mexico Geological Society Guidebook, Albuquerque Country II.

Xu, M., and Eckstein, Y., 1995, Use of weighted least squares method in evaluation of the relationship between dispersivity and field scale, GroundWater 33, no. 6:905-908.

Zheng, C., 1990, A modular three-dimensional transport model for simulation of advection, dispersion, and chemical reactions of contaminants in groundwater systems, S.S. Papadopulos and Associates, Inc., prepared for the U.S. EPA Robert S. Kerr Environmental Research Laboratory.

Zheng, C., and Wang, P.P. 1999, MT3DMS, A modular three-dimensional multi-species transport model for simulation of advection, dispersion and chemical reactions of

contaminants in groundwater systems; documentation and user's guide: U.S. Army Engineer Research and Development Center Contract Report SERDP-99-1.

EPA United States Environmental Protection Agency